Chem Soc Rev

REVIEW ARTICLE

View Article Online
View Journal | View Issue

Cite this: *Chem. Soc. Rev.*, 2019, **48**, 2338

Design, synthesis, and biomedical applications of synthetic sulphated polysaccharides

Hannah E. Caputo, [a] John E. Straub [a] and Mark W. Grinstaff *[abc]

Sulphated polysaccharides play important roles in a number of physiological and patho-physiological processes including the coagulation cascade, viral transmission, and antioxidation. In nature, sulphated polysaccharides are highly diverse, possessing variations in the carbohydrate backbone, location of the sulphate group(s), and degree of sulphation. These compositional attributes lead to varied sulphated polymers with different negative charge densities and resultant structure–property–activity relationships. Sulphating naturally occurring polysaccharides and their synthetic analogs is challenging, and traditionally requires harsh conditions and long reaction times, often causing non-selective sulphation at different and/or multiple hydroxyl positions. In this Review, we begin with a discussion of both established and novel methods and reagents for sulphation of these polymers, along with the advantages and disadvantages of these various approaches. Next, we describe characterization methods to confirm sulphation. Finally, we provide examples of synthetically sulphated natural polysaccharides and sulphated synthetic polysaccharides, and discuss the utility of these novel polymers in various biomedical applications. This review provides a comprehensive analysis of synthetic sulphated polysaccharides, their current uses, and highlights biomedical opportunities.

Received 1st September 2017

DOI: 10.1039/c7cs00593h

rsc.li/chem-soc-rev

Introduction

Sulphated polysaccharides perform diverse roles in biology acting as structural components of tissue to signaling agents in physiological processes.[1–4] As such, their composition and structure, as well as their physicochemical, biomechanical, and biological properties are of keen interest for basic studies and for development of new products in the pharmaceutical, medical device, food, beauty, and health industries.[6–9] The activity of

[a] *Department of Chemistry, Boston University, 590 Commonwealth Avenue, Boston, MA 02215, USA. E-mail: mgrin@bu.edu*
[b] *Department of Biomedical Engineering, Boston University, 44 Cummington Avenue, Boston, MA 02215, USA*
[c] *Department of Medicine, Boston University, 75 Francis Street, Boston, MA 02215, USA*

Hannah E. Caputo

Hannah E. Caputo received her Bachelor's degree from University of New Hampshire in 2014. She is pursuing a PhD degree under the mentorship of Professors Mark W. Grinstaff and John E. Straub. Her research interests lie in the synthesis, characterization, and modelling of sulphated polysaccharide analogs.

John E. Straub

John E. Straub is a Professor of Chemistry and Materials Science at Boston University. His awards include the Alfred P. Sloan Research Fellow and the Metcalf Award for Excellence in Teaching. John has published more than 140 peer-reviewed publications and given more than 200 oral presentations. He investigates fundamental aspects of protein dynamics and thermodynamics underlying the formation of protein structure, through folding and aggregation, and enabling protein function, through pathways of energy flow and signaling.

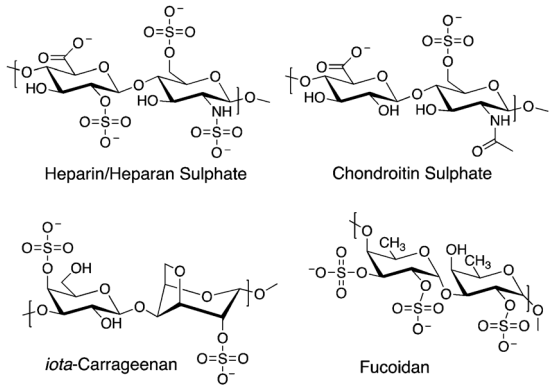

Fig. 1 Structures of various natural sulphated polysaccharides.

sulphated polysaccharides depends on the carbohydrate backbone composition, molecular mass, and, importantly, the position of sulphation and amount or degree of sulphation (Fig. 1). Natural sulphated polysaccharides display both branched and linear polymer architectures. The biological activities of natural sulphated polysaccharides include: anticoagulation, anti-thrombotic, antiviral, antioxidant, antitumor, anti-inflammatory, antiatherosclerotic, anti-adhesive, antipeptic, antiulcerogenic,[10,11] antilipidemic,[2] and lubricity, and are highly dependent on structure and composition. These activities arise from discreet polysaccharide–protein interactions (*e.g.*, anticoagulation) as well as coordination and storage of water (*e.g.*, lubricity). Some common natural sulphated polysaccharides are fucadion, carrageenan, heparin, and chondroitin sulphate (Fig. 1), and their corresponding biological functions are summarized in Table 1.

The presence of a sulphate group on the polysaccharide structure affords a number of chemically important outcomes. First, the sulphate group possesses a negative charge over a wide pH range (4–12) in order to electrostatically bind to positively charged biomolecules. For example, the glial cell-derived neurotropic factor (GDNF) binds to sulphated polysaccharides, and is responsible for the survival and differentiation of dopaminergic neurons.[12,13] Second, the sulphate group coordinates water molecules to increase and maintain tissue hydration. For example, the presence of sulphated and carboxylated glycosaminoglycans (GAGs) in articular cartilage maintain hydration, compliance, and elastohydrodynamic lubrication. GAG depletion increases hydraulic permeability and reduces resistance to compressive loads, thereby compromising its functional performance, leading to an osteoarthritic state.[16] Furthermore, multiple sulphates on a single polysaccharide promote an open extended solution conformation structure to minimize electrostatic repulsion between the negative charges. Finally, sulphated polysaccharides are negatively charged polymers, which do not alter pH, unlike carboxylated polysaccharides.

Given the interesting and diverse biological activities of sulphated polysaccharides, significant research efforts are on-going to synthesize sulphated polysaccharides *via* the step-wise addition of sugars,[17,18] and to develop structure–property–activity relationships. However, the synthesis of sulphated polysaccharides is challenging due to the large number of stereocenters, the presence of similar functional groups, and the need to preserve the orientation of glycosidic linkages. Preparing both small and large molecular weight polymers with narrow polydispersity creates an additional challenge. Therefore, from a chemical synthesis perspective, polymeric sulphated structures are obtained by sulphating either natural polysaccharides or polymeric analogs of polysaccharides. These post-polymerization modification approaches are efficient and can provide ample material for biological assays and for comparative studies to naturally occurring sulphated polysaccharides.

We begin with a discussion of both traditional and recently published methods to sulphate polysaccharides, analysing the scope and reactivity along with advantages and disadvantages of these methods, followed by relevant characterization methods. Next, we describe several examples of natural polysaccharides that have been synthetically sulphated and examples of entirely synthetic sulphated polysaccharide analogs. Finally, we explore the diverse biological activities of these sulphated polysaccharides and analogs in order to understand the structure–activity relationship of sulphated polysaccharides. This review will not discuss the sulphation, synthesis or biological activities of sulphated non-polysaccharide or non-carbohydrate polymers, and the reader is referred to several excellent reviews on this specific topic.[22,23] Overall, this review provides a comprehensive analysis of the methods for sulphation, insight into the structure–activity relationship of sulphated polysaccharides, and highlights the key sulphation characteristics, site of sulphation, and degree of sulphation responsible for the observed biological activity.

Mark W. Grinstaff

Mark W. Grinstaff is the Distinguished Professor of Translational Research, a Professor of Biomedical Engineering, Chemistry, Materials Science and Engineering, and Medicine at Boston University, and the Director of BU's Nanotechnology Innovation Center. Grinstaff's groundbreaking research has yielded more than 300 peer-reviewed publications, and more than 200 patents and patent applications. He is a co-founder of five companies and his innovative ideas and efforts have led to several new commercialized products. His research interests cover a broad range of topics but always with an emphasis on new compositions, synthetic methods, and evaluation of properties.

General sulphation methods

There are several challenges associated with polysaccharide sulphation, including the low reactivity of the hydroxyls, the poor solubility of the polysaccharides in organic solvents, the maintenance of the glycosidic linkage, the regioselectivity and

Table 1 Various natural polysaccharides, their structural differences, and biological activities

Name	Sugar residue/monomer unit	Biological activity(s)	Natural source	Ref.
Carrageenan	Galactose units and 3,6 anhydrogalactose	Anticoagulant, antithrombic, antioxidant, antiviral, antitumor, immunomodulatory	Red algae	5
Ulvan	Rhamnose, xylose, iduronic and glucuronic acids	Anticoagulant, antioxidant, immunomodulatory, anti-inflammatory, antilipidemic	Green algae	2 and 14
Heparin/heparan sulphate	2-*O*-Sulphated iduronic acid and 6-*O*-sulphated, *N*-sulphated glucosamine	Anticoagulant and antithrombotic	Porcine intestine, bovine lung	15
Chrondoitin sulphate	*N*-Acetyl galactosamine and glucuronic acid	Osteoarthritis, and anti-inflammatory	Cornea, cartilage, bone	19
Calcium spirulan	*O*-Rhamnosyl-acofriose and *O*-hexuronosyl-rhamnose (aldobiuronic acid)	Antiviral, and anti-herpes	Sea algae	20 and 21
Kerate sulphate	Lactosamine	Tissue hydration	Cornea, cartilage, bone	24
Fucan/fucoidan	Mainly fucose	Anticoagulant, antithrombotic, antitumor, immunomodulatory, anti-inflammatory, antilipidemic and anticomplementary properties, activity against hepatopathy, uropathy and renalpathy, gastric protective effects	Brown algae	25
Dermatan sulphate	Hexosamine, *N*-acetyl galactosamine and glucuronic acid	Anticoagulant, and antithrombic	Bone, cartilage	28

amount of sulphation, and the isolation of the product. As there are only a few solvents that both the polysaccharide and the sulphated product are typically soluble in, reactions tend to not reach completion. Identifying and subsequently targeting a specific sulphation site is difficult due to the multiple hydroxyls present on the polysaccharide. Consequently, protecting groups are required, which increases the synthetic complexity and the total number of reactions, decreasing overall yield. Sulphating multiple hydroxyls on a single carbohydrate repeat unit provides an additional challenge due to electrostatic repulsion between neighbouring sulphates. Sulphated polysaccharides are usually isolated as salts; again, adding a layer of complexity to the procedure. As such, significant research efforts are directed towards sulphation of both natural and synthetic polysaccharides,[26] and below we summarize the advantages and limitations of current methods.

Sulphur trioxide complex reagents

Currently, the most widely employed method for the sulphation of a polysaccharide is to use sulphur trioxide–amine complexes in a highly polar organic solvent such as dimethylformamide (DMF) or dimethylacetamide (DMA) (Fig. 2). The advantages of sulphur trioxide complexes include their relatively stability, ease of handling, and compatibility with highly polar solvents aiding in the solubility of polysaccharides.

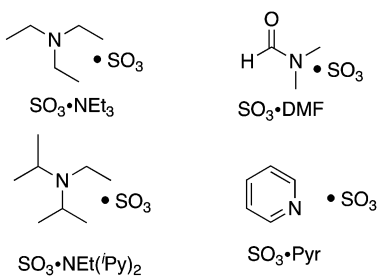

Fig. 2 Sulphur trioxide complexes with amines.

For example, the Li group[27] used three different sulphation methods to sulphate polysaccharides isolated from pumpkin. The later two methods are described in following sections with different reagents. In the first method, the sulphation reagent was prepared by dissolving sulphur trioxide (1.0 g) in pyridine (20 mL). The polysaccharides were dissolved in DMF, followed by the addition of the sulphation reagent and subsequent stirring at 60 °C for 10 hours. Next, the reaction solution was diluted with DI water, neutralized with 2.5 mM NaOH, dialyzed, and freeze-dried to afford the sulphated polysaccharide fractions. This method gave a high percent yield, 118% w/w yield, and a high degree of sulphation: 3.4% sulphur content or 0.20 degree of sulphation (DS).

Richter and coworkers[29] reported the regioselective sulphation of trimethylsilyl cellulose using sulphur trioxide complexes. Specifically, they investigated whether sulphation of fully substituted trimethylsilyl cellulose with SO_3·DMF, SO_3·Pyr, SO_3·NEt_3, or SO_3·$NEt(^iPy)_2$ resulted in sulphated cellulose as shown in (Fig. 3). All reactions were run in tetrahydrofuran (THF) at room temperature for 24 hours with 2.2 equivalents of the SO_3 complex per mol of monomer. The proposed mechanism for sulphation involves insertion of the sulphur into the oxygen–silicon bond, followed by loss of trimethylsilanol in basic work up. After purification by multiple precipitations in methanol, ethanol, and acetone, the products were dialyzed and freeze-dried. The different sulphur trioxide complexes gave moderate to good percent yields between 60–75%. Specifically, the use of SO_3·NEt_3 afforded the lowest degree of sulphation (DS = 1.01), with a 64% yield. The SO_3·DMF reagent was the most reactive

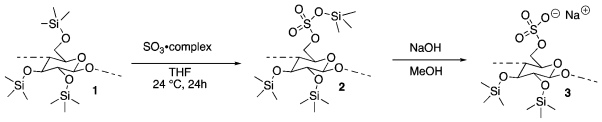

Fig. 3 Sulphation of trimethylsilyl cellulose (TMSC) with SO_3-complexes.

Table 2 Degree of sulphation (DS) of sodium cellulose sulphates prepared from trimethylsilyl cellulose (TMSC) and SO_3 complexes (25 °C, 24 h; NaOH/MeOH work-up)

	DS		
SO_3·complex (2.2 mol eq.)	Total[a]	O-6[b]	O-2[b]
SO_3·DMF	1.88	0.95	0.51
SO_3·DMF	1.75[c]	0.95[c]	0.50[c]
SO_3·DMF	1.57[d]	0.95[d]	0.44[d]
SO_3·DMF	0.95[e]	0.68[e]	0.22[e]
SO_3·pyridine	1.31	0.62	0.42
SO_3·NEt(^{i}Py)$_2$	1.23	0.54	0.49
SO_3·NEt$_3$	1.01	0.21	0.44

[a] According to elemental analysis. [b] Determination by ^{13}C-NMR spectroscopy. [c] Reaction time 8 h. [d] Reaction time 7.5 h. [e] Reaction time 4 h.

reagent and its use gave the highest degree of substitution (DS = 1.88), 75% yield. Sulphation *via* the SO_3·NEt(^{i}Py)$_2$ and SO_3·Py reagents resulted in degrees of sulphation of 1.23 and 1.31, and yields of 60% and 72%, respectively.

The regioselectivity of these sulphation reactions was also studied. The selectivity ratio decreased from predominantly O-6 sulphation over O-2 sulphation to both O-6 and O-2 sulphation for the SO_3·DMF reagent as the total degree of substitution increased with time (Table 2). Additionally, SO_3·DMF regioselectively sulphated the O-6 position ($DS^{O\text{-}6}$ = 0.95; $DS^{O\text{-}2}$ = 0.51) whereas SO_3·NEt$_3$ sulphated the O-2 position preferentially ($DS^{O\text{-}6}$ = 0.21; $DS^{O\text{-}2}$ = 0.44). No significant selectivity for a sulphation site was obtained with the SO_3·NEt(^{i}Py)$_2$ and SO_3·Py reagents. None of the reaction conditions afforded significant sulphation at the O-3 position. These results provide three important findings for controlling the site of sulphation:

(1) Steric interactions hinder the substitution of secondary positions (O-2 and O-3) relative to the primary positions (O-6).

(2) The polarity of the O–S bond in the SO_3 is influenced by electron transfer effects between the sulphur atom and the nitrogen atom of the amine, which are controlled by the amine substituents.

(3) The O-2 hydroxyl of the anhydroglucose is the most acidic due to the electronic effects of the glycosidic bond and the O–Si bond in position O-2 is the most polar.

These results suggest that the regioselectivity of the sulphation reaction is not only influenced by steric effects, which would favour O-6 sulphation, but is influenced by electronic effects as well, as seen in the sulphation with SO_3·NEt$_3$, which selects for O-2 site. Here, triethylamine acts as an electron donor, increasing the polarity of the S–O bond in SO_3 that approaches the most polar Si–O bond in position O-2.

Microwave-assisted sulphur trioxide complex method

Desai and coworkers[30] investigated microwave irradiation as an alternate reaction procedure for sulphur trioxide sulphation using sulphur trioxide amine complexes. In acetonitrile, a series of small molecules, including one monosaccharide, were sulphated with yields greater than 90% in 20–30 minutes (Fig. 4). The increased reaction rate is likely due to the rapid heating generated during the microwave process. The reactant/sulphated product may couple to

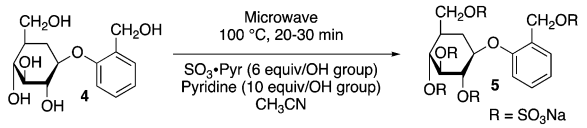

Fig. 4 Microwave assisted sulphation of monosaccharide.

microwaves through ionic conduction in acetonitrile,[31] converting the microwave irradiation energy into heat, evenly heating the reaction mixture faster than a traditional oil bath method. Acetonitrile was used as it allows for good solubilisation of the product and its easy isolation due to its low boiling point. Conducting the reaction in DMF and nitromethane, both microwave compatible solvents, decreased the reaction percent yields significantly to 17–23%. Addition of a free base (Et_3N) to the reaction in acetonitrile increased the yields from 5% with no free base to 80% with 5 equiv. (per –OH group). Further increasing the Et_3N to 10 equiv. resulted in only a small increase in the yield. Desai further evaluated sulphur trioxide complexes of trimethyl amine and pyridine, and found that the pyridine complex nearly doubled the yield for two of the substrates, including the saccharide, to 84% yield, when compared to the SO_3·NMe$_3$. Based on this observation, the proposed sulphation mechanism involves a general base catalysis rather than a deprotonation followed by a nucleophilic attack, as pyridine is a weaker base than Et_3N and does not deprotonate the OH immediately. Advantages of this procedure include: (1) compatibility with a range of functional groups such as aldehydes, esters, ethers and amides; and (2) sulphation of multiple hydroxyls including alcoholic and phenolic hydroxyls in one step to obtain per-sulphated products in relatively high yields. While this method was only investigated with small molecules, its success suggests utility for sulphating polysaccharides.

Chlorosulphuric acid (CSA)

Traditionally, sulphation of polysaccharides is accomplished using sulphuric acid and chlorosulphuric acid (Fig. 5) to generate an active sulphur trioxide reagent.[32] Yoshida and coworkers[33] sulphated curdlan to study its inhibitory effects against HIV-1 and HIV-2. For the sulphation reaction, curdlan (0.5 g) was added to chlorosulphonic acid (CSA) (4.4 g) in dry pyridine (80 mL) and was stirred for 1 hour at 100 °C. The reaction mixture was diluted with 10% NaOH, dialysed, and freeze-dried to obtain the sulphated curdlan (1.22 g) with 19.4% sulphur content.

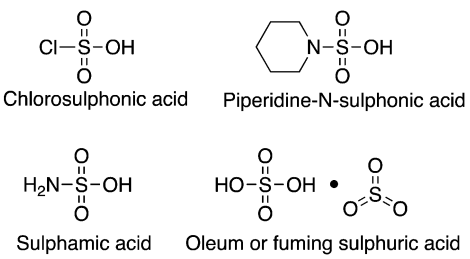

Fig. 5 Structures of different sulphation reagents.

CSA-pyridine reagent

The Li group[27] also used the CSA-pyridine reagent to sulphate polysaccharides isolated from pumpkin. The sulphation reagent was prepared by slowly adding CSA to pyridine at 0 °C, followed by stirring continuously for 40 minutes at 0 °C and then at room temperature for an additional 30 minutes. The resulting sticky white sulphation reagent was added to the polysaccharide (dextran and pullulan)[34] in formamide at 60 °C for 4 hours. Next, the reaction mixture was neutralized by NaOH, dialysed against DI water, precipitated in ethanol, and freeze-dried to give sulphated pumpkin polysaccharides. This method gave slightly lower percent yields, 115% w/w, and degrees of substitution (3.27% sulphur content or 0.19 DS), than the sulphur trioxide pyridine method described earlier.

Sulphamic acid-pyridine

The sulphamic acid-pyridine reagent was also used to sulphate natural polysaccharides by the Li group.[27] Sulphamic acid (0.5 g) was dissolved in pyridine (20 mL) to generate the sulphation reagent. The polysaccharide was dissolved in DMF and after addition of the sulphation reagent, the reaction was stirred at 60 °C for 10 hours. The reaction was then diluted with DI water, neutralized with 2.5 mM NaOH, dialyzed, and freeze-dried to afford the sulphated polysaccharide. This method gave lower yields and degrees of sulphate substitution than both the sulphur trioxide pyridine and CSA-pyridine methods, with 91% w/w yield, and a DS of 0.02. Cellulose has also been sulphated using sulphamic acid in DMF at 80 °C.[35] However cellulose is known to degrade upon heating with sulphamic acid, but addition of urea, acting as a base catalyst, allows the sulphation reaction to occur with less degradation.[36]

Sulphamic acid was also used by Zhou and coworkers[37] to sulphate natural polysaccharides isolated from corn bran. The extracted corn bran polysaccharides (CBPs) were dissolved in DMF (60 mL) and sulphamic acid (2.0 g) was added drop wise. The reaction was stirred at 90 °C for 2.5 hours and then cooled in an ice bath to obtain sulphated CBPs with DS values between 4.61 and 5.55.

Piperidine-*N*-sulphonic acid

Curdlan[33,38] and dextran[39,40] have been sulphated with piperidine-*N*-sulphonic acid,[41] which is a milder sulphation reagent often resulting in less product degradation. Uryu and coworkers[40] sulphated a branched dextran by dissolving the polysaccharide in dimethylsulfoxide (DMSO), adding piperidine-*N*-sulphonic acid (448 mg), and heating at 85 °C for 1 hour. After cooling in a water bath, sodium bicarbonate (7 mL) was added to quench the reaction. The reaction mixture was then dialysed and lyophilized to obtain a sulphated dextran (91.5% yield) with a DS of 1.34.

Oleum

Oleum, or fuming sulphuric acid is a solution of sulphur trioxide in sulphuric acid, and was used in 2005 by Varlamov and coworkers[42] to sulphate chitosan. The sulphating agent was prepared by adding small aliquots of oleum to DMF while stirring vigorously at 0–5 °C. The chitosan was added and the sulphation reaction was conducted at 60 °C for 1–3 hours. The reaction was then cooled to room temperature, and the product was crystallized in acetone and purified on a Sephadex G-10 column to give 0.4–1.2 g of sulphated chitosans with varying DS between 0.83–1.66.

DMAP/DCC catalysed CSA reaction

To address the challenges of slow reaction rates and degradation during the sulphation reaction, Wang and coworkers[43] developed a catalytic method using 4-dimethylaminopyridine (DMAP) and *N*,*N*-dicyclohexylcarbodiimide (DCC). Using the CSA and pyridine method for sulphation of *Artemisia sphaerocephala* polysaccharide (ASP), a natural polysaccharide, a catalytic amount of DMAP and DCC was added to the reaction. Both DMAP and DCC are common catalysts for esterification, silylation, carbamolyation, sulphonylation, and phosphorylation reactions.[44] Increasing the quantity of DMAP from 0 to 10 mg increased the DS values of sulphated polysaccharides from 0.51–0.87 to 1.01–1.28. However, the amount of DCC did not affect the DS, as it was used as a dehydration agent forming dicyclohexylurea (DCU) which precipitated.[45] Increasing the temperature from 60 °C to 90 °C only resulted in more degradation instead of greater DS or yields. Sulphation of ASP was confirmed through FT-IR, and ^{13}C NMR, with percent yields between 74 and 117% w/w. Other research groups have utilized DMAP to catalyse sulphation reactions on a variety of polysaccharides.[46–48]

Sulphation in ionic liquids

Sulphation reactions are typically performed in polar organic solvents such as DMF, DMSO, or pyridine. Sulphating polysaccharides in these solvents is challenging due to poor solubility, the requirement of longer reaction times, and the use of higher temperatures. These conditions along with the acidic sulphation reagent or by-products often degrade the polymer backbone. Ionic liquids (ILs) are enticing alternative solvents that, due to their miscibility with water and organic solvents, readily dissolve polysaccharides, potentially reducing the required reaction time and temperature.

Lui and coworkers[47] investigated the sulphation of polysaccharides isolated from the herb, *Momordica charantia* L. (MC) in ionic liquids. The sulphated MCP derivatives (MCPS) were sulphated with CSA/pyridine in IL 1-butyl-3-methylimidazolium chloride ([C4mim]Cl), with DMAP and 1-(3-dimethylaminopropyl)-3-ethylcarbodiimide hydrochloride (EDC·HCl). MCP (100 mg) was added to [C4mim]Cl (1000 mg) at 80 °C and stirred for 1 hour, before addition of the sulphation reagent. Then 30 mg of DMAP and 30 mg of EDC·HCl were added and the reaction was stirred at 70 °C for 1 hour. The mixture was subsequently cooled to room temperature, neutralized with 2.5 M NaOH, and purified by dialysis for 24 hours. Five different MCPSs were obtained with DS between 0.72–1.13. Other research groups have had similar success with sulphation reactions on polysaccharides in ionic liquids.[46]

Cyclohexyl sulphate protecting group

Sulphated structures are often difficult to isolate and handle because they are prepared as the free salt form and are only

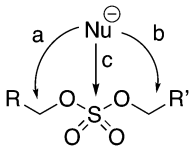

Fig. 6 Nucleophilic attack on a sulphate diester.

soluble in water. For this reason, sulphation reactions are frequently performed as the last step in a synthetic route. To address this limitation Perlin and Penney[49] reported the first protecting group for sulphates in 1981. The roles of a sulphate-protecting group are to: (1) mask the anionic charge of the sulphate; (2) increase the solubility of the protected polysaccharide in DMF or other organic solvents; and (3) be readily cleaved. One approach is to use a diester; the resulting sulphate diesters, however, are unstable and highly susceptible to nucleophilic attack at three different positions. As shown in Fig. 6 substitution by route (**a**) is generally slow when R is a carbohydrate. Therefore the goal is to choose R′ such that the nucleophilic substitution is disfavoured by route (**b**), but reactive enough for selective removal to give the sulphate monoester.

Perlin and Penney described the use of phenyl sulphates. A partially protected monosaccharide was reacted with phenyl chlorosulphate to afford the corresponding phenyl sulphocarbohydrate (77% yield). The phenyl protecting group was removed *via* hydrogenation of the phenyl ring to a cyclohexyl group under excess potassium carbonate and catalytic platinum-oxide/H_2 in methanol/water. While the authors did not report yields for this deprotected product, the protecting group was further cleaved in basic conditions, yielding only moderate sulphate formation.

Trifluorodiazoethane sulphate protecting group

Flitsch and coworkers[50] developed the trifluoroethyl ester protecting group for sulphate esters in 1997, to address the limitations involved with the use of the cyclohexyl protecting group. The trifluoroethyl ester protecting group was selected since it had been previously used to protect carboxyl and phosphate groups. The group is selectively removed using Zn/AcOH. The one step reaction involves addition of 2,2,2-trifluorodiazoethane with citric acid in acetonitrile and stirring at RT for 24 hours. A number of protected monosaccharides including, fructose, glucose and galactose, were successfully sulphated at either the 2, 3, 4 or 6 position in reasonable to good yields (46–93%). The trifluoroethyl protecting group is stable under conditions commonly used to deprotect carbohydrates including strong acids, hydrogenation conditions, sodium methoxide, and TBAF, as well as high temperatures (refluxing methanol). The sulphate-protecting group is removed in excellent yields (82–96%) by refluxing with potassium *tert*-butoxide in *tert*-butanol in 1–2 hours.

Trifluoroethanol imidizole protecting group

Taylor and coworkers[51,52] developed a new protecting group for sulphates: a sulphate monoester, which avoids the use of the reactive and toxic trifluorodiazoethane. It contains a trichloroethanol (TCE) protecting group on the sulphate and a positively charged imidazole leaving group for reactivity with a hydroxyl.

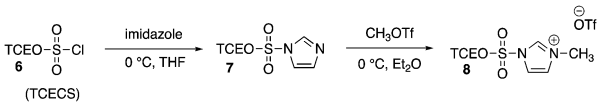

Fig. 7 Synthesis of sulphuryl imidazolium triflate.

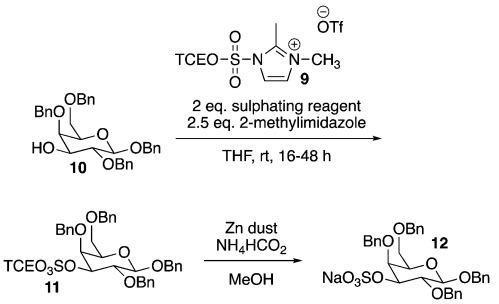

Fig. 8 Sulphation conditions with TCE sulphating reagent and TCE deprotection.

The TCE sulphating reagent is readily prepared by reacting sulphuryl chloride with 1 eq. 2,2,2-trichloroethanol in the presence of 1 eq. pyridine in ether to obtain 2,2,2-trichloroethyl chlorosulphate (TCECS **6**). TCECS reacts with 1 eq. of imidazole to give the imidazolium product **7** in 86% yield. The imidazolium triflate salt **8** precipitates from solution during the following triflation reaction with methyl triflate in dry ethyl ether in near quantitative yield (Fig. 7). Using a derivative of this reagent **9**, a wide variety of monosaccharides with different protecting groups were sulphated in the presence of 2-methyl imidazole in THF at room temperature for 16–48 hours. Although diisopropylidene-D-galactose was used as a model substrate, other investigated monosaccharides included tetra-benzylated galactose and diacetoneglucofuranose each with the O-3 hydroxyls free and various glucopyranosides with combinations of protecting groups leaving free hydroxyls at the 2, 3, 4, or 6 position for sulphation. The monosaccharides were all sulphated with the above reagent in excellent yields (81–94%) and the TCE group was removed using zinc ammonium formate in methanol in similarly excellent yields (91–99%) (Fig. 8). The TCE group is stable under conditions commonly used in carbohydrate chemistry including the removal of acetate esters and benzylidene acetals. The removal of benzyl groups in the presence of the TCE group was performed under photochemical conditions, initially reported by Brinkley,[53] as standard hydrogenolysis conditions (Pd/C, $H_{2(g)}$) resulted in removal of the TCE group. More recently, the Taylor group utilized this reagent for *N*-sulphations[52] and multiple sulphations[54] on monosaccharides but, as of yet, this reaction has not been investigated for the sulphation of polysaccharides. Overall this methodology has the potential to significantly impact the sulphation of carbohydrates.

Alkyl sulphate protecting group

Simpson and Widlanski[55] developed alkyl protecting groups for sulphates, installed as sulphate diesters, that are stable to conditions including reductive and nucleophilic reagents. Neopentyl and isobutyl groups were chosen as protecting groups as they are primary aliphatic groups that are unreactive

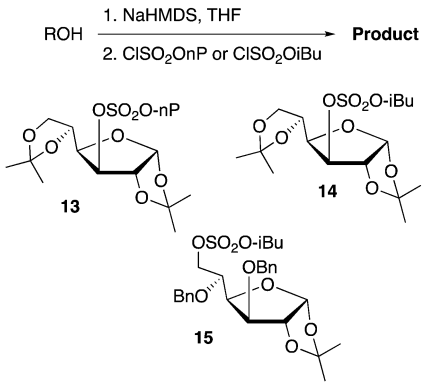

Fig. 9 Synthesis of alkyl protected sulphate monoesters. *^{i}Bu = isobutyl, nP = neopentyl.

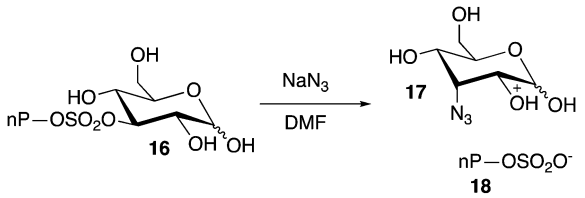

Fig. 10 Reaction of sodium azide with aliphatic neopentyl-protected sulphate monoester.

to nucleophilic conditions. Neopentyl groups are known to be extremely stable, requiring high temperatures and long reaction times for removal.[56] Isobutyl groups are easier to remove but less stable to nucleophilic conditions.[57] The neopentyl and isobutyl chlorosulphates were easily prepared by the reaction of the respective alcohols with sulphuryl chloride.[58] Carbohydrates were then treated with sodium hydride or sodium bis(trimethylsilyl)-amide (NaHMDS) in THF with 20% *N*,*N*′-dimethylpropyleneurea (DMPU) at −75 °C followed by slow addition of the sulphation reagent to yield the sulphate protected carbohydrate (95–99% yield) (Fig. 9). Nucleophilic conditions in a polar aprotic solvent were used to remove the neopentyl and isobutyl protecting groups. The high stability of the neopentyl group required a small nucleophile, such as azide for complete removal. However, the specific conditions required to remove the neopentyl group resulted in azide substitution of the substrates, revealing that this method was not useful for sulphation of carbohydrates (Fig. 10). Removal of the isobutyl group proceeded successfully with sodium iodide in hot acetone at 55 °C in excellent yields 96–97% (Fig. 11).

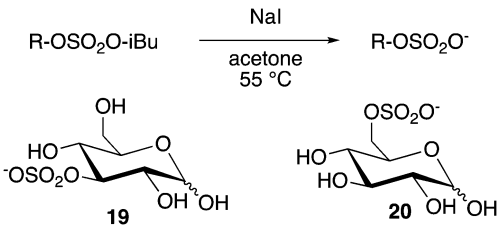

Fig. 11 Deblocking isobutyl protecting groups.

Chemoenzymatic synthesis using sulphotransferases

Liu and co-workers[59] utilized a chemoenzymatic method to synthesize low molecular weight heparin (LMWH) on a gram scale as 12-mers, improving upon the previous milligram scale.[60,61] The chemoenzymatic synthesis of two dodecasaccharides, 12-mer-1 (**21**) and 12-mer-2 (**22**) was completed in 22 steps with 10.3% overall yield and 23 steps with 8.2% overall yield respectively. For the sulphation steps, *N*-sulphotransferases (NST), 2-*O*-sulphotransferases (2-OST), 3-*O*-sulphotransferases (3-OST) and 6-*O*-sulphotransferases (6-OST) were utilized in 12 different steps to install the 17 and 18 sulphate groups for **21** and **22** respectively. The structures of **21** and **22** differ in only one 3-*O*-sulphate group present in the 12-mer-2 at residue G and not present in 12-mer-1 (Fig. 12).

Boons and co-workers[62] developed a controlled chemoenzymatic synthesis that employs chemically synthesized oligosaccharides **23–25** (Fig. 13). These hexasaccharides were treated with *N*-sulphotransferases (NST) in the presence of 3′-phosphoadenosine-5′-phosphosulphate (PAPS) to give the di-*N*-sulphated derivatives with yields between 60–80%. These derivatives as well as hexasaccharides **23–25** were subjected to C5 epimerases (C5-Epi) and varying sulphotransferases (NST, 2-OST and 6-OST) providing a library of 21 different oligosaccharides varying in *N*/*O*-sulphation and epimerization pattern. In order to achieve high fidelity in the chemoenzymatic synthesis, they methylated the C6 hydroxyl group of a glucosamine residue to block specific enzymatic transformations.

Characterization methods

Post sulphation, the degree of sulphation (DS) and the position of sulphation on the polysaccharide or monosaccharide must

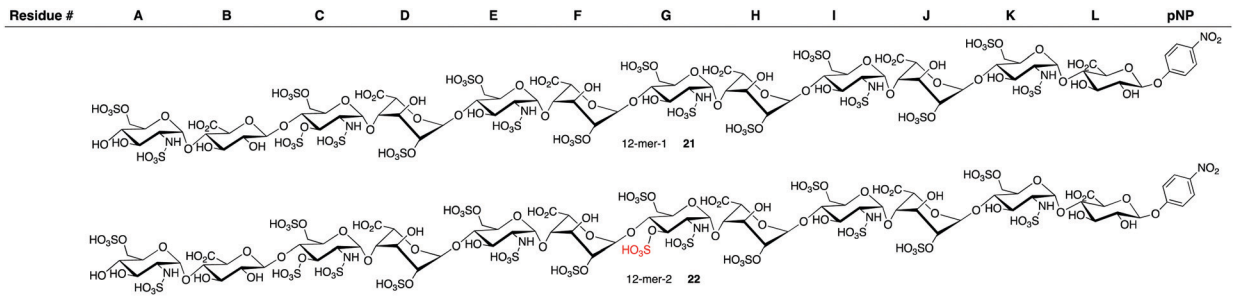

Fig. 12 Chemical structure of 12-mers.

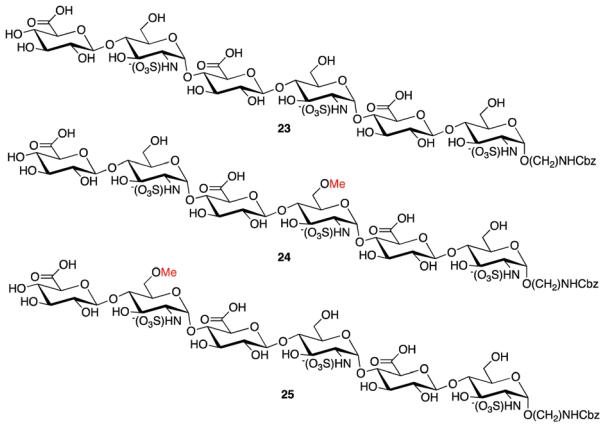

Fig. 13 The hexasaccharides **23–25**.

be determined. A number of analytical techniques and methods are used to characterize sulphated derivatives as described below. Traditional methods for the determination of sulphate content in polysaccharides including gravimetric estimation of barium sulphate,[63] colorimetric benzidine sulphate,[64] titration with barium chloride,[65] spectrometric estimation using barium chromate, and 4-amino-4′dichlorobiphenyl methods[66] have been previously described and will not be discussed below. Instead infrared and Fourier-transform infrared spectroscopy (FTIR) spectroscopy, ^{1}H and ^{13}C nuclear magnetic resonance (NMR) spectroscopy, gel permeation chromatography (GPC), toluidine blue analysis, azure A analysis, elemental analysis, benzidine method, and barium chloride–gelatin nephelometric techniques will be discussed along with computational modelling to provide additional insight into the structure and conformation of sulphated polysaccharides.

Infrared and FTIR

IR spectroscopy is a common analytical method used to confirm the installation of sulphate groups on polymers, due to its sensitivity, quick readout, and minimal sample requirement.[67] The SO_2 group possess several IR active vibrational modes including asymmetric and symmetric absorption bands (ν_{asym} and ν_{sym}) at 1270–1200 cm^{-1} and 1060–1010 cm^{-1}, respectively, a SO_2 scissoring mode at 600–590 cm^{-1}, and the C–O–S stretching vibration at 900–800 cm^{-1}. In IR analysis, one typically measures the ν(S=O) (1270–1200 cm^{-1}) and ν(C–O–S) vibrations (880–800 cm^{-1}) as these vibrations are the strongest and easily identifiable.

Recently, the Lajunen group reported the IR spectra of several different sulphated polysaccharides.[68] The wavenumber of the ν(C–O–S) vibration depends on the position of the sulphate substituent. In various sulphated 3,6-anhydrogalactose samples, the vibrations for the secondary sulphate positions (4 or 2) appear at higher frequencies (850–840 cm^{-1} and 840–825 cm^{-1} respectively) than the vibrations of a primary sulphate group at position 6 (820–810 cm^{-1}). Additionally, when the polysaccharide contained multiple sulphate groups a broad band is observed between 850–800 cm^{-1}.

Quantitative IR spectroscopy can also be performed using a calibration curve to determine the amount of sulphate group as the intensities of the IR absorption bands are proportional to the number of vibrating groups/bonds.[69,70]

^{1}H and ^{13}C NMR

Although the sulphate group is not directly detectable by ^{1}H and ^{13}C NMR, the proton or carbon signals of the adjacent CH or CH_2 shift when a sulphate group is attached. The Lajunen group[68] also reviewed NMR studies of common natural polysaccharides, including amylose, cellulose, curdlan, chitin, chitosan, pectin, and carrageenans, as well as their own synthetic sulphated polysaccharides to analyse the differences in the ^{1}H and ^{13}C NMR spectra. In sulphated polysaccharides, the protons adjacent to the *O*-sulphate groups are shifted slightly downfield (0.46–0.83 ppm) relative to the non-sulphated hydroxyl. For ^{13}C NMR, the downfield shift of the carbon bound to the *O*-sulphate groups is more apparent (4.5–8.5 ppm) compared to the carbons not bound directly to *O*-sulphate which shift slightly upfield (0.1–2.0 ppm),[71] as exemplified for cellulose and chitosan sulphates. Overall ^{13}C NMR data provides more information for determining the sulphate position, as there is less signal overlap and a greater shift in the sulphated derivatives. However, it is not the most efficient method, due to the longer relaxation times that are required for polysaccharides and is used sparingly.

Gel permeation chromatography

Gel permeation chromatography (GPC), also known as size exclusion chromatography (SEC), is a useful technique to determine the molecular weight of polymers when compared to a calibration curve derived from standards of known molecular weights. However typical polymeric standards are not sulphated, and, thus, there is significant error in estimating the molecular weight. While GPC cannot directly confirm sulphation, the retention time before and after sulphation changes significantly due to the introduction of charge on the polymer.[72]

Toluidine blue

The reagent 'toluidine blue' is used to determine the sulphate content on large molecular weight sulphated polysaccharides.[73,74] Toluidine blue is a positively charged basic thiazine metachromatic dye that stains polysaccharides purple (Fig. 14). In a typical procedure, an exact amount of the dry sulphated polymer is immersed in a known volume of known toluidine blue and the absorbance at 560 nm is measured *via* a UV-vis spectrophotometer. By measuring the absorbance of the sulphated polysaccharide (*e.g.*, hyaluronic acid) and comparing the absorbance values to a calibration curve obtained by measuring solutions of known amounts of sulphate salts, the number of sulphate groups on the polysaccharide are determined.

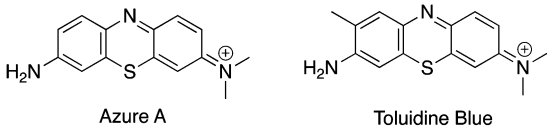

Fig. 14 Structures of Azure A and toluidine blue.

Azure A analysis

Azure A is also used to assess the degree of sulphation in a manner similar to that of toluidine blue (Fig. 14).[75] Azure A is a coloured positively charged small molecule that, when mixed with a negatively charged sulphated polysaccharide, exhibits a decrease in light absorption at 620 nm. Again, using a standard curve, the absorbance of the Azure A–polysaccharide complex is correlated to the amount of sulphation.[76]

Elemental analysis

A reliable method to determine the amount of sulphation is elemental analysis. With this method, the average amount of sulphate per mass of polymer or small molecule is determined. If one knows the molecular weight of the polymer, the average amount of sulphates per monomer is estimated as a percentage. The equation below is used to convert the sulphate content percentage (S%) to degree of sulphation (DS), which represents the average number of sulphates on monomer residues.[46] However, this method does not identify the position(s) of the sulphate group(s) or the exact number of sulphates present per monomer.

$$\mathrm{DS} = \frac{1.62 \times S\%}{32 - 1.02 \times S\%}$$

Benzidine method

One of the most common methods for determination of sulphate content is the benzidine method developed by Antonpoulos[77] in 1962. As a colorimetric method, it is more accurate than gravimetric methods. First, the polysaccharide is hydrolysed in 25% formic acid for 24 hours to release all the sulphate groups. Then, the hydrolysate (0.3 mL), 95% ethanol (0.5 mL), 0.2 mL benzidine reagent (0.5% benzidine in 95% ethanol) and amyl alcohol (0.5 mL) are all combined in a conical centrifuge tube. The tubes are shaken and left at 0 °C for 1 hour before being centrifuged for 6 min. The supernatant is carefully removed and discarded, and then 1 mL of acetone–ethanol (1 : 1) and 0.5 mL of amyl alcohol are added. The tubes are shaken again and re-centrifuged for 6 min. This step is repeated once more without addition of amyl alcohol. After three rounds of centrifuging, the precipitate is dissolved in 2 mL of distilled water and 3 mL of 1.0 N HCl. Addition of 1 mL of 0.1 N sodium nitrite diazotizes to the benzidine solution affords the bis(diazonium) salt. After three minutes, 5 mL of thymol solution (0.5% w/v thymol in 2 N NaOH) is added and the tubes are shaken. The absorbance is measured in a 1 cm cell at 505 nm, and as before, the sulphate content is derived by comparison to a standard curve.

Barium chloride–gelatin nephelometric method

The Zhou group determined the percentage of sulphate in their sulphated polysaccharides *via* the barium chloride–gelatin nephelometric method.[27] This method was first developed in 1974 by Tabatabai[78] to measure the sulphate content in water samples. The method is based on measuring the turbidity formed when an aliquot of the barium chloride–gelatin reagent is mixed with an aliquot of acidified water containing sulphate. The reagent is simply a mixture of gelatin (0.6 g in 200 mL water) and barium chloride (2.0 g). The sample to be analysed is taken as a 20 mL aliquot and combined with 2.0 mL of 0.5 N HCl and 1.0 mL of the barium chloride–gelatin reagent. After 30 minutes, the turbidity of the solution is measured. The amount of sulphate is calculated by comparing to a calibration curve, which is obtained using the turbidity of mixtures of known concentrations of potassium sulphate with the reagent. This method has been used to determine the sulphate content of both polysaccharides[27,79] and small molecules.

Computational modelling

Computational modelling offers valuable insight into the structure and chemical properties of molecules and macromolecules. Remko and coworkers utilized quantum mechanical calculations to determine the conformational structures of the α-L-iduronic acid,[80] dimeric,[80] trimeric,[81] and pentameric[81] units of heparin. They applied appropriate theory levels and basis sets (B3LYP/6-31+G(d)) to study the interactions between the negatively charged sulphate and carboxylate groups in heparin with the positively charged sodium ions present in solution. From these studies the lowest energy conformation with sodium ions was determined which contained multidentate coordination bonds with Na^+ from the carboxylate and sulphate groups. Computed pK_a values of the sulphate, carboxylate, and hydroxyl groups were determined to be pK_a = 0.25 for C2 sulphate groups, pK_a = 3.67 for C5 carboxylate and pK_a = 14.00 for C3 hydroxyl. Therefore at physiological pH = 7.4, both the sulphate and carboxyl groups are fully ionized. Remko also studied the effect of different metal ions in water on the conformational changes in Fondaparinux.[82] When Fondaparinux is coordinated with different cations, Li^+, Na^+, K^+, Mg^{2+}, and Ca^{2+} ions, only slight conformational changes were noted.

Previously, carbohydate force fields were used to examine specific sulphation patterns.[83] Mallajosyula and Mackerell *et al.* developed new parameters and extended the methodology to *N*- and *O*-sulphation.[84] These parameters enable the investigation of structural and dynamic properties of sulphated polysaccharides in solutions using molecular dymanics (MD) simulations. These parameters are also compatible with the existing Chemistry at Harvard Macromolecular Mechanics (CHARMM) protein force field, which is a widely used set of force fields for MD. Simulations of phosphate monosaccharides and sulphated polysaccharides demonstrated the compatibility between CHARMM and the newly developed parameters. The parameter development methodology included transfer of charge and non-bonded parameters from existing CHARMM phosphate and sulphate parameterizations. The crystallography-identified contacts and contact probabilities from the simulations were in excellent agreement, demonstrating the force field's ability to maintain key crystal contacts. The expansion of the CHARMM biomolecular force field utilized here, allows for further computational studies of sulphated polysaccharides and other complex heterogeneous biological systems.

Hünenberger and co-workers[85] developed a new parameter set (45A4) for the GROMOS force field specifically designed for simulations of explicit-solvent hexopyranose-based carbohydrates. The previous parameter sets (45A1 and 45A3) underestimated the

anomeric effect and gave incorrect dihedral-angle distributions in simple disaccharides, sometimes distorting their ring conformations. The charges and torsional interaction parameters were refined in the new GROMOS 45A4 force field. These parameters were validated by comparison to available experimental data from X-ray crystallography and NMR spectroscopy of a small set of mono- and disaccharides. Simultaneously, van Gunsteren and co-workers[86] developed a similar parameter set (53A6) to account for the same deficiencies. The GROMOS 45A4 force field was successfully used to investigate the stability of amylose and cellulose fragments after methylation at specific hydroxyl groups.[87] Seven years later, Lins and co-workers[88] described an improved parameter set for GROMOS, referred to as $53A6_{GLYC}$, with the intent to expand the GROMOS 45A4/53A6 force field to other biomolecules, including proteins, lipids, and nucleic acids. The addition of two torsional potentials overcame the limitation in previous parameters of adequate description of the preferred aldohexopyranose puckering conformations. The new parameter set $53A6_{GLYC}$, was validated by comparison with NMR data of 16 different monosaccharides and eight different disaccharides. Further refinement of the GROMOS force field is being investigated to extend to other carbohydrates, including acetylated sugar derivatives and furanoses.

Woods and co-workers developed a new derivatization of the GLYCAM force field parameters (GLYCAM06) that removes its specificity for carbohydrates and extends its use to all molecular classes.[89,90] They also validate the GLYCAM force field parameters for modelling GAGs.[91] Specifically, Woods compared NMR data and MD simulations for variably sulphated disaccharides and two sulphated tetrasaccharides to determine the ring structure and glycosidic linkages of the oligosaccharides. The transferable sulphate model in GLYCAM allows it to be applied to multiple attachment points without the development of separate charge sets, simplifying the process. These works improved the accuracy of the MD simulations, validating the force field parameters for future work on sulphated GAGs. For more information on computational work on GAGs and their protein interactions, please see the following reviews.[92–94]

Sulphated natural polysaccharides: synthesis and biological activities

Sulphation of natural polysaccharides is a relatively quick and efficient approach to synthesize sulphated polysaccharides, as one is using a previously isolated polysaccharide. Therefore, this is a common approach to synthesize sulphated polysaccharides for research studies and applications. In the following subsections, various biomedical applications are described where sulphated natural polysaccharides demonstrate biological activity.

Anticoagulants

Anticoagulants are used for a wide variety of hospital procedures and surgeries to control bleeding and clotting. Of the natural sulphated polysaccharides, heparin, primarily composed of uronic acid and glucosamine subunits, is a widely used anticoagulant[95–98] having an annual market of 7 billion dollars.[99] In fact, one third of hospitalized patients in the USA, about 12 million each year, receive heparin.[100] Discovered in 1916,[101] it is clinically used for the treatment of thrombic disorders by minimizing blood clotting *via* enhancing the rate at which antithrombin inhibits proteases in the coagulation cascade.[95] Pharmaceutical-grade heparin is commonly isolated from the mucosal tissues of porcine or bovine, and it naturally exists in a wide range of molecular weights and carbohydrate subunit sequences, both of which affect its bioactivity. Unfractionated heparin (UFH) is the full-length form,[102] and low molecular weight heparin (LMWH)[103] is a depolymerized heparin form that has predictable pharmacological properties, making it more useful for clinical use. The LMWHs currently on the drug market are Enoxaparin,[104] Dalteparin,[105] and Tinzaparin.[106] Due to its structural complexity and size, all of heparin's roles *in vivo* are challenging to identify and study. Crystal structure analysis of the heparin and antithrombin III complex[107–111] identified a pentasaccharide fragment with specific sugar residues responsible for its activity.[112] Although widely used,[100] alternatives for heparin are of keen interest, and as such, significant research efforts are underway to develop and test synthetic anticoagulants.

The Ducatti Group[113] regioselectively sulphated three different carrageenans and investigated their anticoagulant activity in an activated partial thromboplastin time (aPPT) *in vitro* assay. They isolated kappa-, iota-, and theta-carrageenans from natural sources, cyclized the structures under basic conditions, and regioselectively sulphated the polysaccharides at different positions. From the three carrageenans investigated, eight different sulphated products were obtained, with differing degrees of sulphation at different positions (Fig. 15). The polysaccharides were sulphated *via* SO_3·pyridine in DMF at 20 °C for 1 h to obtain sulphated cyclized carrageenan diads. Triethyl amine and 2-methyl-2-butene were added to decrease depolymerization products. These sulphated polysaccharides and one non-sulphated carrageenan were evaluated using the aPTT assay for anticoagulation activity (Fig. 16). The carrageenans, with higher degrees of sulphation (DS = 3.8), gave higher anticoagulation activity – a longer time to clotting. In addition, sulphation at the C2 of the anhydro-α-D-gal and the C6 of the β-D-gal increased the anticoagulation activity.

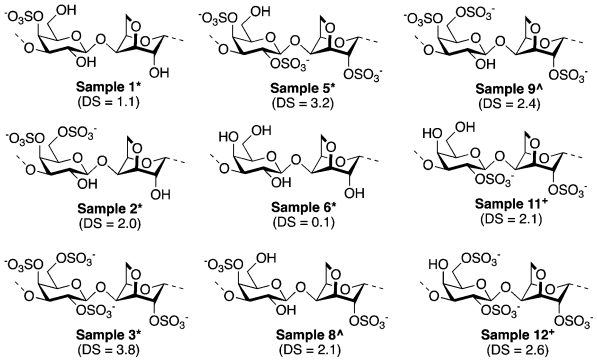

Fig. 15 Structures of sulphated and de-sulphated carrageenans *from kappa-carrageenan, ^from iota-carrageenan, +from theta-carrageenan with degree of sulphation (DS).

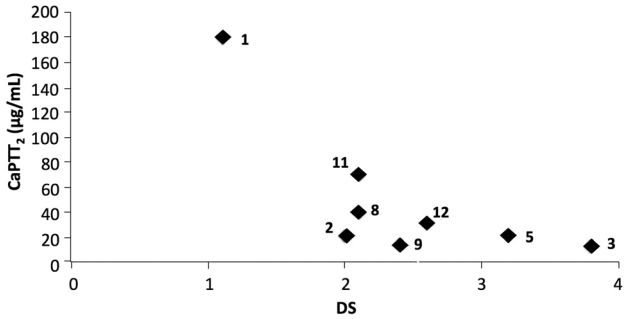

Fig. 16 Dependence of the degree of sulphation (DS) and sample concentration required to double aPTT of saline ($CaPTT_2$) for sulphated carrageenans. *Numbers correspond to the sample numbers in Fig. 15. Adapted with permission from C. A. de Araujo, M. D. Noseda, T. R. Cipriani, A. G. Goncalves, M. E. Duarte and D. R. Ducatti, *Carbohydr. Polym.*, 2013, **91**, 483–491. Copyright 2012, Elsevier publishing.

Toida and coworkers[114] sulphated (1→3)- and (1→4)-linked natural polysaccharides including xylan, cellulose, amylose, curdlan and galactan, and investigated their anticoagulation properties against antithrombin III and Factor IIa. The polysaccharides were successfully sulphated using SO_3·pyridine (15 equiv. per hydroxyl group) in DMF at 40 °C for 6 hours to give DS of 2.1–2.9. The sulphation reaction was repeated until the polysaccharides were fully sulphated, with a sulphate on all free hydroxyls. The anticoagulant activities of the fully sulphated and specially 6-desulphated polysaccharides were determined *via* the amidolytic method.[115] Normal human plasma (30 μL) was incubated with the sulphated polysaccharides (50 μL) in 50 mM Tris–HCl buffer with 227 mM NaCl and human thrombin (20 μL) for 30 seconds at 25 °C. Then 50 μL of chromozym TH (tosyl-glycyl-proplyl-arginine-4-nitanilide acetate) was added, and the absorbance was measured at 405 nm with a UV-vis spectrophotometer (Fig. 17). The measured activity was compared to heparin (172 units per mg). The polysaccharides exhibited anticoagulation activities between 26.4–42.0 units per mg, except for the sulphated galactan (2.8 units per mg). Since anti-thrombin III and heparin cofactor IIa are both present in human plasma, additional studies investigated thrombin activity independently in plasma-free systems and with purified antithrombin. The sulphated polysaccharides failed to inhibit thrombin in these studies, leading to the conclusion that the observed anticoagulation activity in the amidolytic assay is *via* heparin cofactor II and not through anti-thrombin III.

The Du group[116] studied the structure–anticoagulant activity of sulphated and carboxylated lacquer polysaccharides and the effect of the carboxylate group and the position of sulphation. Lacquer polysaccharides were isolated from sap and either sulphated directly using SO_3·pyridine in DMSO[117] at 60 °C for 3 hours (DS 1.57), oxidized at the primary 6 position to carboxylates using (2,2,6,6-tetramethylpiperidin-1-yl)oxyl (TEMPO), or oxidized and subsequently sulphated (DS 1.11). The anticoagulant activity was measured *via* the standard aPTT assay using normal human plasma. Interestingly, the oxidized polysaccharides shortened the aPTT (34.8–31.0 s) compared to the control (40.6 s), therefore promoting the intrinsic coagulation pathway (Fig. 18). The sulphated and oxidized polysaccharides showed weak anticoagulant activity that increased with higher DS (from 43.0 s to 61.0 s). For sulphated polysaccharides lacking carboxylates, however, the aPTT increased from 80.9 s to greater than 1200 s with DS from 0.8 to 1.57.[118] These results indicate that sulphation at the 6 position is important for anticoagulant activity, as the carboxyl group at this position reduced the aPTT. Additionally the sulphated lacquer polysaccharides inhibited thrombin-mediated fibrin formation and the intrinsic coagulation pathway, but not the extrinsic coagulation pathway as determined by results from the aPTT, prothrombin time (PT) and thrombin time (TT) assays.[118] Other groups have sulphated a wide number of natural polysaccharides and utilized either factor IIa/Xa assays, or clotting assays (aPTT, TT, PT) to determine their anticoagulant activity.[42,72,119–127]

Li and co-workers[128] synthesized a fucoslyated nonasaccharide as a novel anticoagulant targeting the intrinsic factor xase complex. Fucoslyated chrondroitin sulphate, isolated from sea cucumber, is a structurally distinct GAG and its nonasaccharide fragment is known to inhibit the intrinsic factor Xase complex (FXase, factor

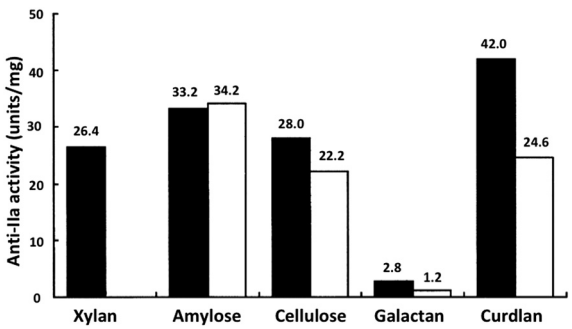

Fig. 17 Anti-IIa activities of chemically fully sulphated polysaccharides and 6-desulphated derivatives. Data were obtained by heparin standard. ■, fully sulphated; □, 6-desulphated, fully sulphated. Adapted with permission from A. Chaidedgumjorn, H. Toyoda, E. R. Woo, K. B. Lee, Y. S. Kim, T. Toida and T. Imanari, *Carbohydr. Res.*, 2002, **337**, 925–933. Copyright 2002, Elsevier publishing.

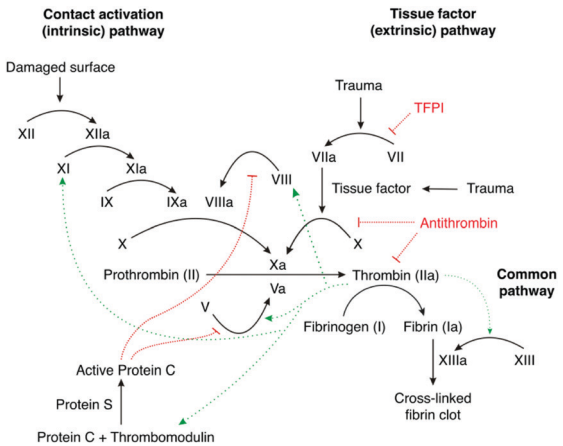

Fig. 18 Anticoagulation pathway. Intrinsic pathway measured by aPTT, extrinsic measured by PT.

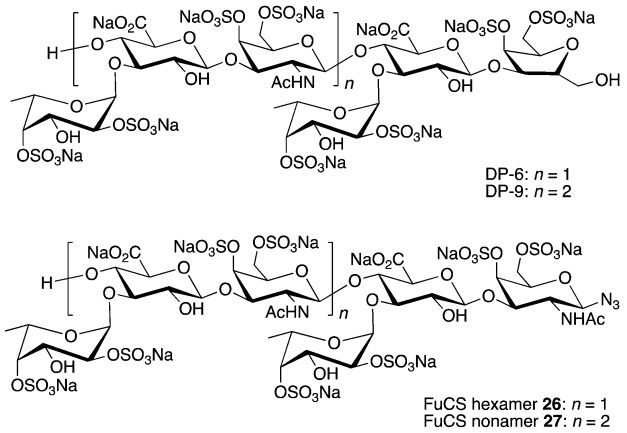

Fig. 19 Structures of depolymerized fragments and FuCS hexamer and nonamer.

IXa-VIIIa complex). For these studies, a method to synthesize the active nonasaccharide fragment was developed from enzymatic degradation of chrondoitin. Chrondoitin was desulphated and degraded to tetra and hexasaccharides, which were used to synthesize the following hexamer and nonamer **26** and **27** (Fig. 19) in 12 linear steps using known saccharide synthesis strategies and sulphated using $SO_3{\cdot}NMe_3$. The anticoagulant activity of **26** and **27** was assessed in comparison to depolymerized fragments, DP-6 and DP-9 (Fig. 19) *via* aPTT, PT and TT plasma clotting assays. FuCS **25** nonamer exhibited potent intrinsic anticoagulation activity, similar to low molecular weight heparin (LMWH), by strongly prolonging the aPTT. To double the aPTT a concentration of 22.73 μg mL^{-1} of **27** nonamer was required, compared to 24.81 μg mL^{-1} (DP-9) and 11.61 μg mL^{-1} for LMWH (Table 3). It also inhibited the factor Xase complex (IC_{50} = 12.9 nM), but did not inhibit factors IXa, XIa or XIIa (Table 3).

In 2007 a supply chain of pharmaceutical heparin was contaminated with oversulphated chondroitin sulphate and was associated with over 200 deaths in the US.[129] The threat of impurities in animal sourced heparin has also triggered the motivation for the preparation of a cost-effective, more structurally defined heparin from non-animal sources. Recently, research groups are utilizing chemoenzymatic methods to synthesize heparin and heparan sulphate oligosaccharides for further biological studies and possible drug development. Linhardt and co-workers[60,61,130] prepared LMWH, ultra-low LMWH and a library of 66 heparan sulphate and heparin oligosaccharides through an efficient chemoenzymatic synthesis method and completed a systematic NMR analysis of the oligosaccharides to obtain a greater understanding of heparin characterization. Specifically, the anticoagulant activity of the 12-mer oligosaccharides (Fig. 12, compounds **21** and **22**) prepared by Liu and co-workers[59] were evaluated *in vitro* in comparison to unfractionated heparin (UFH), fondaparinux, and enoxaparin, an FDA approved LMWH. Both the 12-mer-1 and 12-mer-2 displayed potent anti-factor Xa (FXa) activity with inhibitory concentrations (IC_{50}) of 57 and 67 ng mL^{-1} comparable to UFH 86 ng mL^{-1}. However, neither 12-mer expressed activity against factor IIa (FIIa), and, thus, are specific FXa inhibitors. Lastly, protamine (15 mg kg^{-1}) neutralized the activity of the 12-mer-2 **22** in a mouse model.

Procoagulant

Iacomini and coworkers[131] chemically sulphated mannan and the resultant sulphated polysaccharide possessed procoagulant activity. Mannan was isolated from yeast and chemically sulphated *via* the CSA-pyridine method in formamide at 4 °C for 12 hours. The resulting sulphated mannan (Mn-S1) possessed a DS of 1.66, as determined by the barium sulphate method, and was studied in both *in vitro* and *in vivo* assays for coagulant activity. It exhibited procoagulant activity in a recalcification time study that investigated plasma coagulation without any initiation factor. Following this initial screening, Iacomini evaluated the effect of Mn-S1 on specific proteins in the coagulation cascade. Mn-S1 was shown to inhibit thrombin and factor Xa activity, and therefore to possess anticoagulant properties. A murine model of venous thrombosis was used to determine the *in vivo* effect of Mn-S1. At doses of 0.5 and 1.0 mg kg^{-1} the average dried thrombis weight was 43.5% and 50%, respectively. However at the highest dose of 2.0 mg kg^{-1}, the opposite effect was observed with a 31% increase in the average thrombin formation (Fig. 20). These results warranted further evaluation in an *in vivo* aPTT assay to determine the procoagulant action (Fig. 21). Mn-S1 was administered to rats over a range of doses and circulated for 5 min before blood samples were removed, and the coagulation time was measured. The lowest dose (0.5 mg kg^{-1}) reduced the time by half, while the highest doses clotted immediately on the collection tube, and the time could not be measured. Further studies investigating the apparent procoagulant activity revealed that Mn-S1 activated factor XII, especially at higher doses, and

Table 3 Anticoagulant assays and FXase inhibition activity of **26** and **27**

Compound	MW [Da]	APTT[a] [μg mL^{-1}]	TT[a] [μg mL^{-1}]	FXase[b] [nM]	FXa/AT[b] [μg mL^{-1}]	FIIa/AT[b] [μg mL^{-1}]
26	1952	120.39	>128	>2000	>20 000	>20 000
27	2907	22.73	>128	12.9 ± 0.83	>20 000	>20 000
DP-6[c]	1870	96.13	>128	>2000	>20 000	>20 000
DP-9[c]	2825	24.81	>128	70.5 ± 4.50	>20 000	>20 000
FuCS[d]	68 900	4.30	*ca.* 8–16	0.29 ± 0.02	>2000	282 ± 18.2
LMWH	*ca.* 4500	11.61	*ca.* 4–8	8.77 ± 1.69	89.3 ± 7.77	72.6 ± 4.00

[a] The concentration of each agent that is required to double the APTT or TT; the concentration of all compounds that is required to double the PT is above 128 μg mL^{-1}. [b] IC_{50} value: the concentration required to inhibit 50% activity of FXase, FXa or FIIa. [c] FuCS-derived hexa- or nonasaccharide depolymerized by an *N*-deacetylation-deamination model.[1] [d] Natural FuCS with about 94% 2,4-di-*O*-sulphated fucoses was purified from the sea cucumber *Stichopus variegatus*.

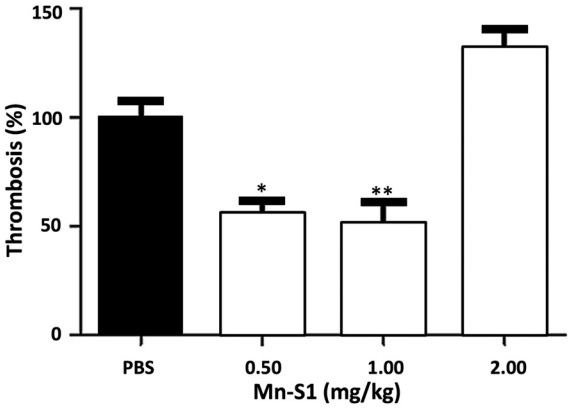

Fig. 20 Venous thrombosis in rats. Thrombin formation was induced by promoting a combination of stasis and hypercoagulability. BS or Mn-S1 were administered at different doses and average dried thrombosis weight was measured. Adapted with permission from A. H. Gracher, A. G. Santana, T. R. Cipriani and M. Iacomini, *Carbohydr. Polym.*, 2016, **136**, 177–186. Copyright 2015, Elsevier publishing.

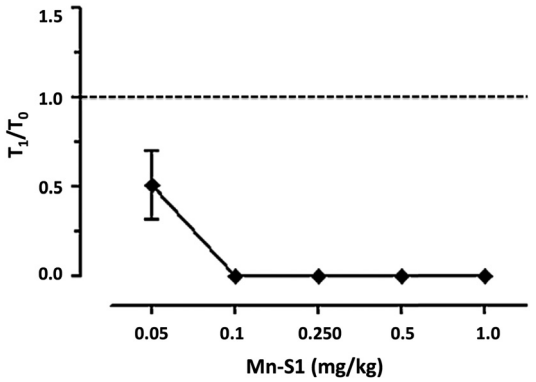

Fig. 21 *In vivo* aPTT, PBS on Mn-S1 at different does were administered in rats and allowed to circulate for 5 min. Results are expressed as T_1/T_0, which is the ratio between the clotting time in the presence (T_1) and absence of polysaccharide (T_0) in the incubation mixture ± SEM (n = 6). Adapted with permission from A. H. Gracher, A. G. Santana, T. R. Cipriani and M. Iacomini, *Carbohydr. Polym.*, 2016, **136**, 177–186. Copyright 2015, Elsevier publishing.

induced platelet aggregation without agonist. Mn-S1 can activate factor XII in the recalcification time study and platelets by acting as a contact surface,[132] explaining its activity as a procoagulant. Conversely, its anticoagulant activity was observed in assays on isolated enzymes that contain numerous positive amino acid residues that bind to the negative charge on Mn-S1.[107] Overall, Mn-S1 demonstrates procoagulant activity, as the concentration of Mn-S1 to activate factor XII is lower than the concentration needed to inhibit α-thrombin and factor Xa. Fonseca *et al.* observed a similar trend with sulphated galactans where low doses (less than 1.0 mg kg^{-1} body weight) gave procoagulant activity while high doses (greater than 1.0 mg kg^{-1} body weight) afforded anticoagulant activity.[133]

Antioxidants

Antioxidants protect cells from damage by reactive oxygen species, such as superoxide anion, hydroxyl radical, and hydrogen peroxide. When these naturally produced oxidizing species are in abundance, a variety of adverse effects occur including carcinogenesis, atherosclerosis, and DNA damage. The Xu group[79] sulphated natural polysaccharides from *D. indusiata* to investigate their antioxidant activity. The *D. indusiata* isolated polysaccharides consisted of glucose units as determined *via* gas chromatography mass spectrometry (GC-MS) analysis of the degraded product. Sulphation of the homopolysaccharide was achieved using the CSA and pyridine method. Three different degrees of sulphation were obtained by controlling the molar ratio of CSA to the monosaccharide residues with ratios of 3 : 1 (S1–DIP), 4 : 1 (S2–DIP) and 5 : 1 (S3–DIP). Sulphation of the homopolysaccharide increased its water solubility in comparison to the original polysaccharide. The presence of sulphate was confirmed *via* FTIR and the barium chloride–gelatin method.[134] The ^{13}C NMR spectrum revealed changes in chemical shifts between the original polysaccharides and the sulphated derivatives consistent with sulphation of one or more of the C-6, C-4 and C-2 positions. Using an antioxidant assay based on scavenging hydroxyl and 2,2-diphenyl-1-picrylhydrazyl (DPPH) radicals, the sulphated polysaccharides were more efficient than the non-sulphated with 65–75% scavenging rate for hydroxyl and DPPH radicals, respectively, compared to approximately 10% for the non-sulphated DIP. The scavenging reactivity increased with greater concentrations of sulphated polysaccharide and degrees of sulphation.

The Du group[117,135] also investigated the antioxidant activities of sulphated lacquer polysaccharides. Hydrolysis of lacquer polysaccharides isolated from the sap of a lacquer tree afforded smaller molecular weight polysaccharides and subsequent treatment with SO_3·pyridine over 4 hours at 60 °C gave sulphated polysaccharides with 0.19 to 0.49 DS. The site of sulphation was proposed to be the 6 position as determined by FTIR analysis.[118] Evaluation of the antioxidant activity *via* superoxide radical scavenging ability and metal chelating activity showed that the sulphated polysaccharides possessed significant antioxidant capacity compared to the non-sulphated control. The potassium ferricyanide reduction method was used to measure the reductive ability and an increase in activity was observed with an increase in sample concentration. The sulphated derivatives quenched superoxide radicals with scavenging percentages between 66.2% and 71.0% compared to 1–2% for the non-sulphated derivatives. Superoxide, a weak oxidant, decomposes to a stronger, reactive oxidative species, so quenching of superoxide radicals is important for anti-oxidation activity. In addition, the sulphated lacquer polysaccharides exhibited increased chelating activity for iron, with 39.3% chelating ability for the polysaccharide with the highest degree of sulphation, 0.49.

Zhou and coworkers[37] studied the antioxidant properties of sulphated corn bran polysaccharides (SCBPs) by investigating their DPPH radical scavenging ability using 2,2′-azino-bis-(3-ethylbenzothiazoline-6-sulphonic acid) (ABTS) and their iron chelating capacity, ICC. The SCBPs exhibited higher DPPH radical scavenging values (47.7–50.2 mg TE per g) (Fig. 22) compared to non-sulphated CBPs (32.7 mg TE per g), which increased with increasing DS. The ABTS scavenging trends increased similar to DPPH with activities between 3.7–4.4 mg

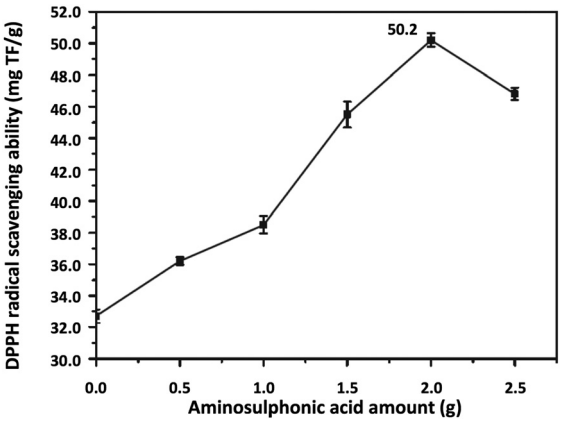

Fig. 22 Antioxidant activity of SCBPs in a DPPH radical scavenging ability study. Adapted with permission from X. Si, Z. Zhou, D. Bu, J. Li, P. Strappe and C. Blanchard, *CyTA–J. Food*, 2016, 1–10, DOI: 10.1080/19476337.2016.1176074, under Creative Commons Attribution 4.0 International license, Nature publishing.

TE per g, higher than the activity for CBP. The iron chelating capacity increased from 8.2 mg TE per g for the non-sulphated CBPs to 12.6–13.3 mg TE per g for the SCBPs. Overall these results demonstrate a significant improvement in antioxidant activity for the SCBPs compared to the non-sulphated CBPs. This result is likely attributed to formation of non-covalent bonds induced by distortion resulting from the introduction of sulphate groups on the hydroxyls. A lengthened chain structure facilitates the interaction with free radicals, and, thus, increases antioxidant activity.[136] The Wang group, who utilized the DMAP/DCC catalyst sulphation method, examined the antioxidant activity of their sulphated ASP and found that the scavenging activities of DPPH, superoxide, and hydroxyl radical all increased with increasing DS.[48,137] Other groups have sulphated natural polysaccharides and studied their antioxidant activities through radical scavenging assays and reducing power assays, and similarly show increased efficacy with increased DS.[47,125,138–140]

Anticancer

The Xu and Chen groups[79] evaluated the cytotoxicity of sulphated polysaccharides, isolated from *D. indusiata* and derivatized using the CSA-pyridine method, on MCF-7 breast cancer cells and B16 melanoma cells using an 3-(4,5-dimethylthiazol-2-yl)-2,5-diphenyltetrazolium bromide (MTT) cytotoxicity assay compared to the non-sulphated controls. For both cell cultures the sulphated polysaccharides showed significant inhibitory effect, while the non-sulphated analogs had no significant effect. Specifically, the sulphated derivatives inhibited growth of MCF-7 and B16 cells by 24% and 48%, respectively, at a concentration of 750 μg mL^{-1}, suggesting that they may possess antitumor activity. Wang and coworkers[141] studied the structure of their sulphated polysaccharides by measuring its chain stiffness *via* viscometry and observed that an increase in chain stiffness gave an increase in antitumor activity. In other studies, it has been demonstrated that sulphation of polysaccharides may be associated with modulation of the host immune system, which contributes to the improvement of the host immunity suppressed by the tumor cells.[142–145]

Zhou *et al.* also investigated the anticancer activity of SCBPs on the cytotoxity of lung (A549) and liver (HepG2) cancer cell lines using an MTT assay.[37] Both cell lines showed a 5–10% decrease in proliferation compared to CBPs with a maximum inhibition of 58.9% and 59.96%, respectively, at 5 mg mL^{-1} (Fig. 23). The molecular mechanism behind the change in proliferation of the cancer cells was studied by measuring the gene expression levels of CASP3, CASP8, CASP9, p53, Bcl-2, and iNOS *via* reverse transcription polymerase chain reaction (RT-PCR). Administration of SCBPs up-regulates CASP3, CASP8, CASP9 and down regulates p53, Bcl-2, and iNOS genes, indicating that the mechanism appears to be linked to activation of apoptotic pathways with enhanced mRNA expression. Other groups have sulphated natural polysaccharides and studied their anti-tumor activities against cancer cells and observe increased anti-tumor activity post sulphation.[46,125,146,147]

Phosphomannopentaose sulphate (PI-88) **28** is a sulphated pentasaccharide originally developed by Parish in 1999,[148] it consists of five mannose units linked with α-glycosidic linkages as shown in Fig. 24. The oligosaccharide phosphate fraction of phosphomannan, produced by yeast *Pitchia (Hansenula) holstii*, is first isolated and then sulphated using the sulphur trioxide-pyridine method described above. PI-88 inhibits the heparanase

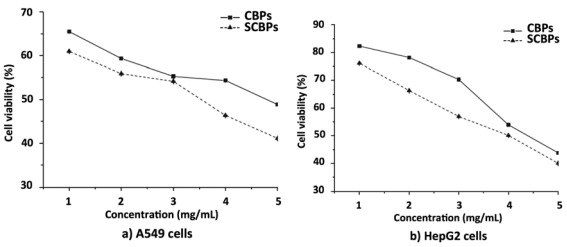

Fig. 23 Cell viability associated with different SCBPs at different concentrations. Adapted with permission from X. Si, Z. Zhou, D. Bu, J. Li, P. Strappe and C. Blanchard, *CyTA–J. Food*, 2016, 1–10, DOI: 10.1080/19476337.2016.1176074, under Creative Commons Attribution 4.0 International license, Nature publishing.

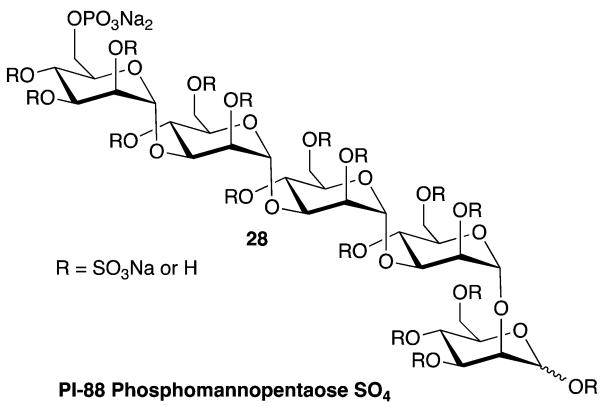

Fig. 24 Structure of PI-88, the lead sulphated oligosaccharide identified by the *in vitro* studies, which was subsequently examined in detail *in vivo* for its antitumor and anti-metastatic properties.

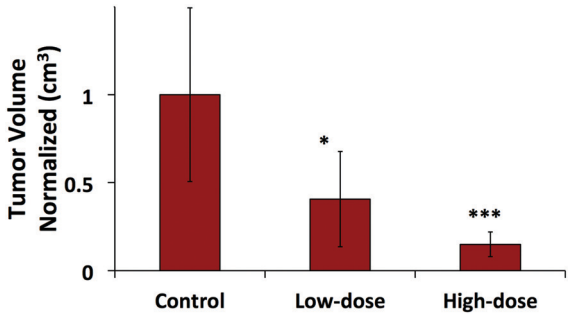

Fig. 25 PI-88 suppressed tumour growth and recurrence in LM3-GFP orthotopic HCC models. Tumour volumes in controls *versus* low- or high-dose PI-88 groups were 0.88 ± 0.18 cm^3 *vs.* 0.35 ± 0.10 cm^3 or 0.12 ± 0.03 cm^3 (P = 0.001). Adapted from B. Y. Liao, Z. Wang, J. Hu, W. F. Liu, Z. Z. Shen, X. Zhang, L. Yu, J. Fan J. Zhou, *Tumor Biol.*, 2016, **37**(3), 2287–2998.

(HPSE) endoglycosidase enzyme inhibitor and has been evaluated in phase I clinical trials for patients with advanced solid malignancies.[149] The clinical trial, reported by Eckhardt and co-workers,[149] determined the maximum tolerated dose (MTD) *via* escalating the PI-88 dose administered subcutaneously (SC) for 4 days per week, along with docetaxel 30 mg m^{-2} given on days 1, 8, and 15 of a 28-day schedule. The MTD of PI-88 is 250 mg per day SC with only mild toxicities of fatigue, diarrhea, nausea and no dose-limiting toxicities (DLTs). Phase II clinical trials, of PI-88, on 41 patients with advanced melanoma gave an overall survival and time to progression similar to standard chemotherapy.[150] Other phase II studies have determined the safety profile of PI-88 to be 160 mg per day with potential to reduce the hepatocellular carcinoma (HCC) recurrence in patients who have had curative resection.[151] Zhou and co-workers[152] investigated the underlying mechanism of PI-88 anti-recurrence and anti-metastasis activity in HCC in both *in vivo* and *in vitro* assays. PI-88 reduced postsurgical recurrence and metastasis of HCC in a mouse orthotopic model of resected HCC. The control group of mice experiences 100% recurrence rate, whereas the rate is reduced to 62.5% for mice treated with PI-88 (20 mg kg^{-1} per day) with a decrease in tumour volumes as seen in Fig. 25. The *in vitro* assays reveal that PI-88 blocks the up-regulation of HPSE after surgical resection. EGR1, a vital transcription factor of HPSE is up-regulated with a surge of growth factors, during the process of liver resection. Overexpression of HPSE enhances the recurrence and metastasis of HCC.[152] For more information on the vascular pathologies of PI-88, please see the following review.[153] Analogues of PI-88 were synthesized by Du,[154] Ferro[155–157] and Ikegami.[158] An efficient synthesis with sequential one-pot glycosidations of PI-88 was also developed by Iadonisi in 2008.[159] The anticoagulant activity of PI-88 has been reported.[160]

Antiviral

Spicer *et al.*[161] investigated the antiviral effect of dextran sulphate, on three different viruses: herpes, encephalomyocarditis (EMC), and Sabin's type 1 polio virus. First, HeLa cells were treated with a medium containing 50 μg mL^{-1} of dextran sulphate, with varying molecular weights, for two days. Both treated and untreated control cultures were infected with varying amounts (0.005 to 5 FPU per cell) of the viruses. The cells were washed to remove any unabsorbed virus after two hours. Twenty-four hours after infection, the cells were lysed (*via* multiple freeze and thaw cycles), and assayed for total virus. Of the three viruses, herpes was most responsive to the treatments with a hundred-fold decrease in virus proliferation *versus* the untreated control. An increase in polymer molecular weight (from 2×10^4 to 200×10^4 g mol^{-1}) afforded inhibition of all three viruses, while the low molecular weight dextran sulphates were active against herpes only. The authors noted that upon treating the HeLa cells with dextran sulphate, the cells aggregated, suggesting that these sulphated polysaccharides are interacting with cell surface receptors. Therefore, Spicer hypothesized that the antiviral effects may be due to the reaction of dextran sulphate with viral receptor sites.

Yoshida and coworkers[33] chemically sulphated curdlan polysaccharides *via* the SO_3·pyridine complex, piperidine-*N*-sulphonic acid, and chlorosulphonic acid methods as described above. All sulphated curdlan polysaccharides prepared exhibited equal antiviral activities against both HIV-1 and HIV-2 as measured by the MTT assay of infected human T-cells. Specifically, MT-4 cells infected with HIV-$1_{HTLV\text{-}IIIB}$ or HIV-2_{ROD} were incubated with various concentrations of curdlan sulphates for 5 days. The curdlan sulphate (DS = 1.4) completely inhibited the infection of both HIV-1 and HIV-2 on MT-4 cells at the EC_{50} of 0.4 μg mL^{-1} and 0.6 μg mL^{-1} respectively. Therefore, the MT-4 cells that were not infected by HIV-1 or HIV-2 proliferated at the same rate as the uninfected MT-4 cells. Other groups have sulphated natural polysaccharides and studied their anti-viral activities against AIDS, HIV-1, HIV-2, Herpes and HSV.[38,121,162–166] Again, similar findings revealed that sulphated natural polysaccharides exhibited high and potent activities against a variety of viruses.

Anti-inflammatory

Wang and coworkers,[167] sulphated polysaccharides isolated from *Cyclocarya paliurus*, an edible plant found in southern China, and studied their anti-inflammatory activity. The polysaccharides were chemically sulphated *via* the chlorosulphonic acid-pyridine method to give sulphated polysaccharides with a DS of 0.42. The inflammatory activity of the sulphated polysaccharides was investigated both *in vitro* and *in vivo*. Nitric oxide (NO) is involved in signal transduction in the immune system and could be produced by a variety of immune cells. Lipopolysaccharides (LPS) are bacterial endotoxins that promote secretion of pro-inflammatory cytokines (IL-1β, and IL-6) as well as increased NO production from cells (Fig. 26). A reduction in NO production may prevent an occurrence of inflammatory diseases.[168] The *in vitro* study examined the nitric oxide (NO) production, IL-1β, and IL-6 secretion and phagocytosis of macrophages in LPS-induced RAW 264.7 cells. The sulphated polysaccharides (S-CP_{1-4}) gave a dose-dependent suppression of NO production as well as a dose-dependent inhibition of IL-1β, and IL-6 production. Using a LPS-injected liver mouse model, intravenous administration of S-CP_{1-4} decreased alanine aminotransferase (ALT) activity in the serum, improved the thymus

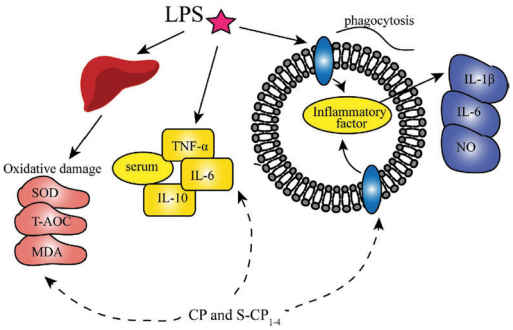

Fig. 26 The possible anti-inflammatory mechanism of CP and S-CP_{1-4}. Adapted with permission from Z. Wang, J. Xie, Y. Yang, F. Zhang, S. Wang, T. Wu, M. Shen and M. Xie, *Sci. Rep.*, 2017, **7**, 40402, under Creative Commons Attribution 4.0 International license, Nature publishing.

and spleen indexes, increased the superoxide dismutase (SOD) activity and total antioxidant capacity (T-AOC) level, and decreased the malondialdehyde (MDA) level. The net effect is an overall increase in anti-inflammatory activity. Wang and coworkers[169] observed similar enhanced anti-inflammatory activity due to suppression of IL-1β and TNF-α with synthetically sulphated Astragalus polysaccharides in Caco2 cells.

Immunomodulating activity

Wang and coworkers,[170] sulphated curdlan *via* the sulphur trioxide·pyridine complex method and the resultant sulphated derivatives exhibited significant immunomodulating activity against murine macrophages and bone marrow-derived dendritic cells (BMDCs). The sulphated curdlans activated RAW264.7 macrophages with increases in IL-6, IL-1β and TNF-α production. This enhanced cytokine production occurred without any observable increases in cytotoxicity.

Growth factor stimulation

Vercoutter-Edouart and coworkers[171] observed enhanced mitogenic activity of human dermal fibroblasts after treatment with dextran sulphates. Platelet derived growth factor (PDGF) is responsible for the growth, migration and differentiation of a wide variety of cells, and is a member of the heparin-binding growth factor family, binding with negatively-charged heparin and glycosaminoglycans *via* electrostatic interactions. Vercoutter-Edouart and coworkers synthesized new dextran derivatives, including dextran methylcarboxylate benzylamide sulphate (DMCBSu) and dextran methylcarboxylate benzylamide (DMCB), and investigated their interactions with PDGF-BB, an important growth factor involved in wound healing. Dextran was sulphated *via* the sulphur trioxide·pyridine complex method in DMSO to give 40 different sulphated dextran derivatives with DS between 0.07–1.26. Agarose gel electrophoresis was used to analyse the effect of the dextran derivatives on the electrophoretic mobility of PDGF-BB. Increasing the sulphate DS (0.07–0.84) enhanced the electrophoretic mobility of the growth factor. PDGF-BB migration also increased when binding with increasing benzylamide DS (0.11–0.47) of dextran methylcarboxylate benzylamide (DMCB). Indicating that the dextran derivatives bound to the PDGF-BB

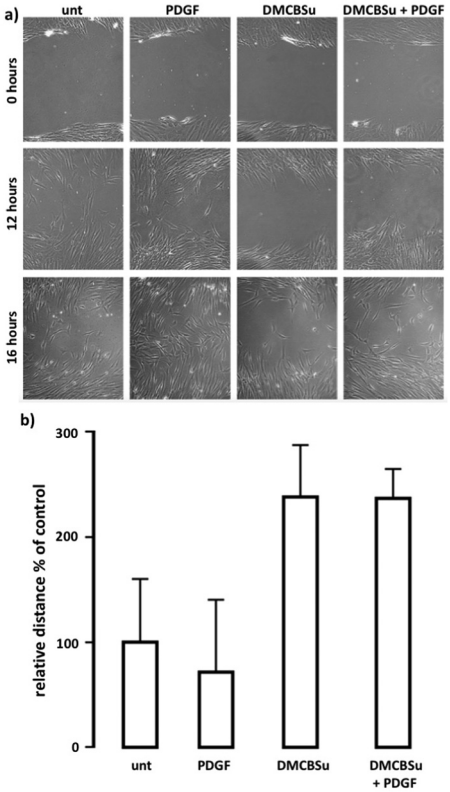

Fig. 27 DMCBSu decreases the early migratory response of HDFs. (a) Phase-contrast micrographs of control cells and cells treated with either 5 ng mL^{-1} PDGF, 2.5 μg mL^{-1} DMBCSu D034, or both were taken after 0, 12, 16 h of treatment. (b) Quantification of the results depicted in (a). Adapted with permission from A. S. Vercoutter-Edouart, G. Dubreucq, B. Vanhoecke, C. Rigaut, F. Renaux, L. Dahri-Correia, J. Lemoine, M. Bracke, J. C. Michalski and J. Correia, *Biomaterials*, 2008, **29**, 2280–2292. Copyright 2008, Elsevier publishing.

growth factor, depending on their DS of both benzylamide and sulphate. To further investigate the effect of DMCBSu in cell migration, a wound scratch assay was performed whereby human dermal fibroblasts (HDF) were grown in monolayers and their ability to migrate to a denuded area was measured over time (Fig. 27). One DMCBSu dextran derivative, D034, with a sulphate DS of 0.29 decreased the early migratory response of HDFs and counteracted the PDGF-stimulatory effect on the migration.

Sulphated synthetic polysaccharides: synthesis and biological activities

Another synthetic approach to sulphated polysaccharides is to synthesize sulphated polysaccharides or polysaccharide mimetics, as opposed to isolating the polysaccharide, and then perform the post-sulphation reaction. The advantages to this method include: (1) greater control over the polysaccharide structure, *via* selection of backbone composition; (2) greater stereochemical control of sulphation positions through protecting group strategies; and (3) fewer unknown impurities. These advantages, however, increase the length of the synthetic route and workload. Yet, the increase

in synthetic control using this approach can facilitate commercial development. Importantly, efforts have yielded commercial successes to include Fondaparinux and Idraparinux.

Anticoagulants

It is suspected that 60–70% of clinical heparin is inactive,[98,172] and constant heparin usage increases virus exposure to patients due to sample contamination as well as undesirable side effects such as bleeding complications and heparin-induced thrombocytopenia (HIT).[95,173] HIT is a potentially devastating condition that activates platelets.[100] It is associated with significant mortality if unrecognized and affects up to 10% of patients, usually occurring within the first 48–72 hours after heparin administration. Unfortunately, HIT often goes unrecognized and undiagnosed in patients because it is so common and can be caused by a wide variety of factors. Therefore, significant research is ongoing to identify fully synthetic alternative anticoagulants to heparin to address these limitations. The chemical synthesis of Fondaparinux and Idraparinux (discussed below), ensures batch-to-batch consistency and the absence of potential risk of contaminations.[174]

Heparin is a highly sulphated, anionic polysaccharide, primarily composed of glucosamine and uronic subunits, the latter consisting of iduronic acid or glucuronic acid residues.[95–98] The challenges associated with synthesizing heparin include: (1) availability of iduronate building blocks, which are rare and commercially expensive;[175] and (2) enabling multiple sequential glycosylations that maintain both anomeric selectivities and high chemical yields. These challenges are compounded when preparing large heparin chains synthetically. To address these challenges, Hansen and Miller[18] first developed an efficient and scalable synthesis of iduronic acid subunits for the disaccharide and tetrasaccharide fragments.[176] Using their tetrasaccharide fragments, a dodecasaccharide was synthesized and sulphated using SO_3·pyridine complex in pyridine at 50 °C for 5 h.[177] The iterative coupling-deprotection two-step homo-ligations of a tetrasaccharide, oligosaccharides afforded the 16-mer to 40-mer.

In 1990 Petitou *et al.* reported[178] a sulphated pentasaccharide (Fondaparinux) as a heparin mimetic based off the five-fragment section of heparin responsible for its anti-coagulant activity, containing both sulphated oxygen atoms and sulphated nitrogen atoms (Fig. 28 and 29). The first synthesis[179,180] was over 40 steps starting from commercially available materials and resulted in less than 1% total yield. In this synthesis, a convergent synthetic

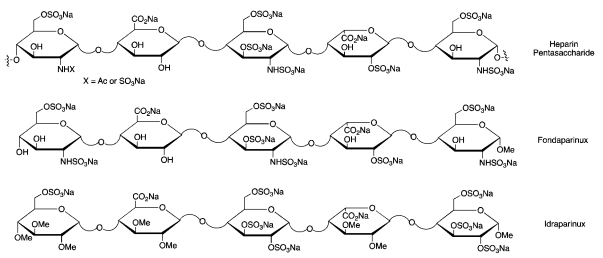

Fig. 28 The anticoagulant pentasaccharide from heparin and synthetic pentsaccharides Fondaparinux and Idraparinux.

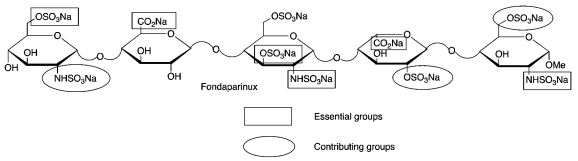

Fig. 29 The essential and contributing groups in fondaparinux sodium for anti-coagulant activity.

strategy was utilized whereby two fragments, one with three sugar units, the other with two units were subsequently linked. The sulphation reaction was the final step in the reaction. To ensure both sulphation sites, Petitou used the following strategy (Fig. 30).[180] Upon completion of the fully protected pentasaccharide, the hydroxyl groups to be sulphated were protected with acyl groups, the nitrogen positions to be sulphated were installed as azides, and the free hydroxyls were protected with benzyl groups. Base catalysed cleavage of the acyl protecting groups followed by sulphation with sulphur trioxide·triethyl amine in DMF resulted in selective *O*-sulphation. This reaction was followed by hydrogenation to remove the benzyl groups and reduction of the azides, followed by sulphation with sulphur trioxide·pyridine in water at pH 9. Using this approach, selective sulphation was accomplished at the nitrogen positions and not the free hydroxyls. Recent reports have described alternative and shorter synthetic routes (>40 to 22 linear steps) to Fondaparinux[181–185] and its analogues.[186] In 2017, a crystal structure of Fondaparinux was obtained[187] and Fondaparinux has been crystallized with antithrombin III.[111,188] Fondaparinux was patented by Choay[189] and Sanofi[190] and marketed in the USA as Arixta® in 2002 by GlaxoSmithKline. The final structure was confirmed by ^{1}H and ^{13}C NMR analysis, and the sulphate modifications slightly shift both the adjacent proton and carbon peaks downfield.[181] There are also examples of ^{15}N NMR on Fondaparinux and heparan sulphate, to study the sulphamate groups and corresponding NH protons in more depth.[191,192] These studies revealed intramolecular hydrogen bonds between the NH proton on the sulphamate group with other sulphate groups in Fondaparinux, particularly the adjacent 3-*O*-sulphate group. The presence of these hydrogens

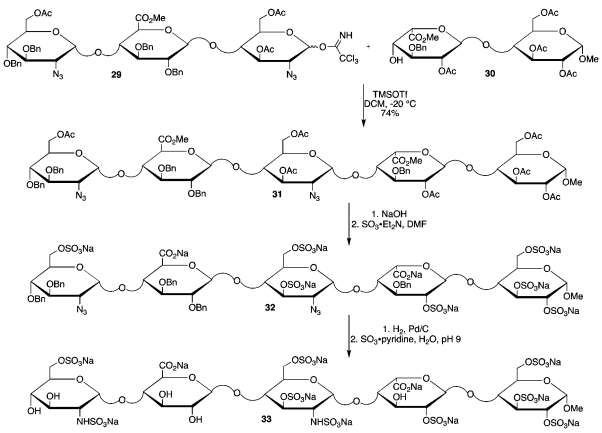

Fig. 30 Final synthesis of Fondaparinux.

bonds have an effect on the conformation of Fondaparinux in solution and suggests that 3-*O* sulphation is important for binding to antithrombin-III.

NMR experiments combined with density functional theory (DFT) calculations provided additional detailed information about the molecular geometry, interactions with solvents and counterions, and formation of both inter- and intra-molecular hydrogen bonds. Hricovini[193] completed both structural and theoretical analysis on Fondaparinux *via* high-resolution NMR and DFT calculations, respectively, to study the molecular structure of this pentasaccharide. Two conformations of the fully optimized molecular structure were obtained, with different conformations of the sulphated iduronic acid residue, using the B3LYP/6-311+G(d,p) level of theory in an explicit water solvent model. Detailed information about bond lengths, bond angles, torsion angles and hydrogen bond formations is further outlined in the paper. The presence of an intra-molecular hydrogen bond between the NH of sulphamate and the adjacent 3-*O*-sulphate group is seen by NMR and DFT optimization. Of the two conformations of Fondaparinux, conformation b (Fig. 31) was determined to be the major conformation, by comparison to experimental data, which differs from the previously published conformation.[194] These data suggest that the protein selects for the more populated $^{2}S_{0}$ conformer, resulting in a binding process that is more energetically favourable than formerly expected.

This pentasaccharide inhibits factor Xa in the presence of anti-thrombin III.[179] It selectively binds to antithrombin III, inducing a conformational change that inhibits factor Xa activity, which decreases thrombin generation.[195–197] Extensive biological studies have revealed the mechanism of action for Fondaparinux's anticoagulation activity. The anti-factor Xa activity of Fondaparinux depends greatly on the assay methodology and experimental procedures. Consequently, Fondaparinux was assigned an arbitrary specific activity of 650 IU mg^{-1} to standardize the expression of dosages for clinical studies. When AT-III is complexed with Fondaparinux, it significantly inactivates factor Xa by about 300 times compared to free or uncomplexed AT-III, signifying the strong anticoagulant activity of Fondaparinux.[198] Clotting studies show that when Fondaparinux was intravenously injected to human volunteers in single administrations of 6, 12 or 18 mg, thrombin generation (TG) and factor Xa activity were inhibited for up to 18 h post injection. Untreated plasma supplemented *in vitro* with Fondaparinux obtained the same anti-Xa activity as the *in vivo* samples demonstrating that Fondaparinux inhibits TG *in vitro* and *in vivo* through the same antithrombin-III mediated inhibition of factor Xa.[199] In standard PT and aPTT clotting assays, Fondaparinux had no effect on the PT time, but slightly prolonged the aPTT time (4–5 seconds).[200] In several thrombosis models in rats, rabbits and baboons, Fondaparinux exhibited potent anti-thrombic activity *via* selective potentiation of factor Xa inhibitory activity of AT-III.[198]

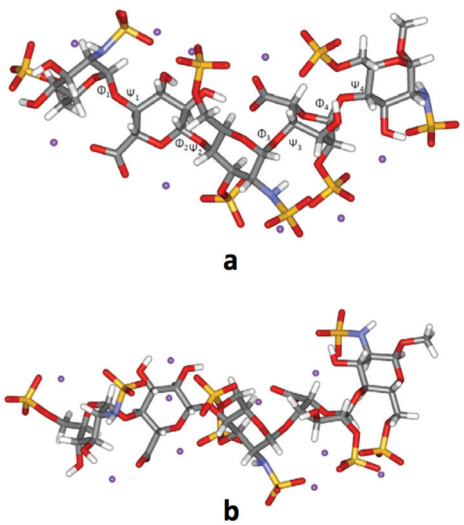

Fig. 31 DFT-optimized structure of heparin pentasaccharide in its two conformations a and b. Adapted with permission from M. Hricovini, *J. Phys. Chem. B*, 2015, **119**, 12397–12409. Copyright 2015, American Chemical Society publishing.

Idraparinux, a fully *O*-sulphated, *O*-methylated heparin mimetic is another synthetic anticoagulant. It exhibits higher anti-factor Xa activity than Fondaparinux, and is considerably easier to synthesize. It possesses a longer *in vivo* half-life (80 h *vs.* 17 h), allowing it to be administered weekly instead of daily.[201] The French pharmaceutical company Sanofi-Aventis first developed Idraparinux. Since its first synthesis, several research groups have developed alternate synthetic routes to idraparinux[201–204] and mimetics.[205,206] However, in all of these strategies, the sulphation reaction and conditions are the same. After completion of the fully protected idraparinux, the pentasaccharide undergoes hydrogenation to remove the benzyl protecting groups followed by sulphation with sulphur trioxide triethyl amine in DMF for 24 hours at either room temperature or 60 °C, giving approximately 70% yield of the sulphated polysaccharide. Idraparinux is a highly selective factor Xa inhibitor that indirectly inactivates factor Xa, by binding to anti-thrombin III in the same manner as Fondaparinux, yet with significantly higher binding affinity.

Unfortunately, Idraparinux did not obtain FDA regulatory approval due to significant complications in the clinical trial. Over the yearlong study, sixteen elderly patients over the age of 75 experienced major intracranial bleeding complications. These complications were thought to be a result of the extended half-life of Idraparinux. Thus, a method was developed to neutralize the anticoagulant effect of Idraparinux by biotinylating the drug (Idrabiotaparinux). The biotin was attached to the C-2 position on the non-reducing end of glucose based on X-ray structural analysis that indicated that this modification site would not disrupt the Idraparinux and antithrombin III interaction. A six-carbon spacer was determined to be the optimal length for the biotin. Avidin, a protein found in egg whites has a high binding affinity for biotin. Thus, administration of Avidin neutralizes the anti-coagulant effect of Idrabiotaparinux, due to Avidin's affinity for biotin. This binding event is used in cases of overdose or bleeding events when the Idrabiotaparinux becomes sequestered. However, Avidin has a half-life of only 2 minutes compared to a half-life of a week for Idrabiotaparinux. As such, anticoagulation returns in the circulatory system. Further clinical

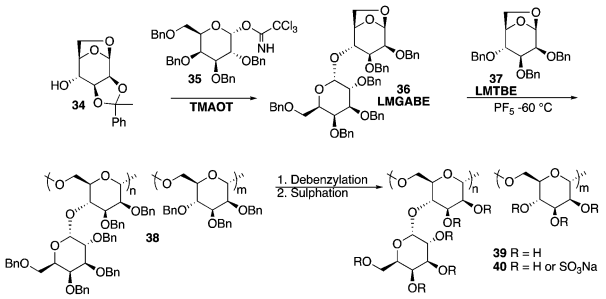

Fig. 32 Synthesis and ring-opening copolymerization of 1,6-anhydro-2,3-di-*O*-benzyl-4-*O*-(2,3,4,6-tetra-*O*-benzyl-α-D-galactopyranosyl)-β-D-mannopyranose (LMGABE) **36** with 1,6-anhydro-2,3,4-tri-*O*-benzyl-β-D-mannopyranose (LMTBE) **37** into stereoregular sulphated synthetic galactomannan **40**.

studies are being completed to analyse the effects of Idrabiotaparinux and its antidote.[207]

Antiviral

Yoshida and coworkers[208] used a new 1,6-anhydro disaccharide to synthesize galactomannan polysaccharides *via* a ring-opening polymerization, which were subsequently synthetically sulphated with the piperidine-*N*-sulphonic acid method. The resulting synthetic sulphated galactomannans exhibited potent anti-HIV activity. Specifically, the disaccharide 6-anhydro-2,3-di-*O*-benzyl-4-*O*-(2′,3′,4′,6′-tetra-*O*-benzyl-α-D-galactopyranosyl)-β-D-mannopyranose (LMGABE) **36** was prepared by glycosylation of 6-anhydro-2,3-*O*-benzylidene-β-D-mannopyranose **34** with 2,3,4,6-tetra-*O*-benzyl-1-*O*-trichloro acetimidoyl-β-D-galactopyranose **35** with TMSOTf, followed by debenzylidenation to recover the hydroxyl groups and subsequent benzylation (Fig. 32). The LMGABE disaccharide monomer is copolymerized with the 6-anhydro mannose monomer, LMTBE **37**, *via* ring-opening polymerization with PF_5 catalyst at −60 °C under high vacuum to give various homo- and co-polymers in good to high yields (47–94%). The polymers were then debenzylated under Birch reduction conditions to give synthetic galactomannans with free hydroxyls in good to excellent yields (50–95%). The sulphation reaction proceeded with piperidine-*N*-sulphonic acid in DMSO yielding the sulphated galactomannans **40** with DS between 1.1 and 1.5. These synthetic polysaccharides were studied for antiviral activity against HIV.[209] The EC_{50} values for the sulphated galactomannans were determined to be between 0.18 to 2.14 μg mL^{-1}, while the CC_{50} were greater than 200 μg mL^{-1} for all samples.

Anticancer

Toshima and coworkers,[142] chemically synthesized five different sulphated tetrafucosides, with differing amounts of sulphation and one non-sulphated tetrafucoside (Fig. 33). The synthetic strategy utilized one common key intermediate with three different protecting groups on the hydroxyls (benzyl, Bn; benzoyl, Bz and *p*-methoxybenzyl, PMP). Orthogonal protecting groups were removed to install sulphate groups at controlled positions, *via* the $SO_3{\cdot}NEt_3$ complex method. The toxic effects of sulphated tetrafucosides on MCF-7 breast cancer cells were studied using

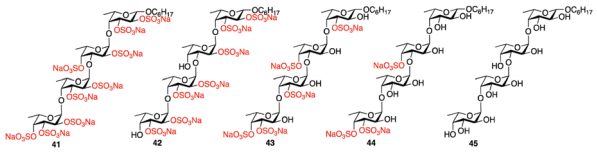

Fig. 33 Structures of synthesized non-sulphated and sulphated tetrafucosides.

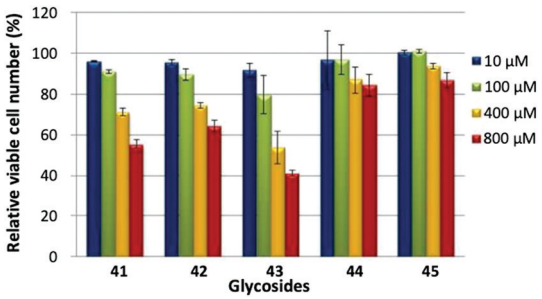

Fig. 34 Effects **41–45** on MCF-7 cell proliferation. Adapted from S. Arafuka, N. Koshiba, D. Takahashi and K. Toshima, *Chem. Commun.*, 2014, **50**, 9831–9834, with permission from the Royal Society of Chemistry.

the MTT assay. The cells were treated with different doses (10–800 μM) for 96 hours (Fig. 34). While the non-sulphated and 4-*O*-sulphated tetrafucosides showed low anti-proliferative activity, the 2,3,4-*O*-sulphated, 2,3-*O*-sulphated and 3,4-*O*-sulphated tetrafucosides effectively reduced the number of MCF-7 cells in a dose dependent manner, with 3,4-*O*-sulphated exhibiting the highest activity.

Glycosaminoglycans

Glycosaminoglycans (GAGs) are sulphated polysaccharides that play a wide variety of biological roles, including ligand recognition and cell signalling processes. GAGs are covalently attached to proteins, and the position and density of these sugar chains impacts the protein–glycan interactions. Significant research is devoted to the design and synthesis of GAGs. Recently, groups are utilizing computational programs to screen potential GAGs for GAG–protein interactions with high-specificity and high-affinity. Using molecular dynamic (MD) simulations Mancera and co-workers investigated the binding of GAGs to endothelial cell adhesion molecule 1 (PECAM-1) and annexin A2.[210] They also, evaluated the application of automated molecule docking and interaction mapping methods to the characterize GAG–protein interactions.[211] Desai and co-workers developed a methodology that identifies potential high-affinity, high-specificity protein–GAG interactions from very large libraries of GAGs and GAG binding proteins.[212–214] The methodology, termed Combinatorial Library Virtual Screening (CVLS) identifies GAG sequence patterns that specifically bind to GAG binding proteins. This information is valuable in the understanding of GAG–protein interactions and in the development of novel therapeutics.

For example, Desai and co-workers[215] utilized their CVLS computational algorithm to scan a library of 46 656 heparan sulphate hexasaccharides to discover and then synthesize a hexasaccharide, containing a rare 2-*O*-sulphate-glucuronic acid

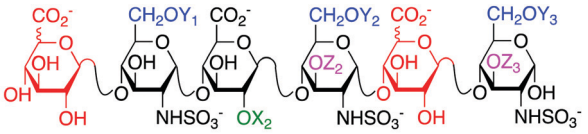

	Residue	Y_1	X_2	Y_2	Z_2	Residue	Y_3	Z_3
HX1	GlcA	SO_3^-	SO_3^-	H	SO_3^-	GlcA	H	SO_3^-
HX2	GlcA	SO_3^-	H	H	SO_3^-	GlcA	SO_3^-	H
HX3	IdoA	H	SO_3^-	SO_3^-	H	GlcA	H	H
HX4	IdoA	SO_3^-	SO_3^-	H	SO_3^-	GlcA	H	H
HX5	GlcA	H	SO_3^-	H	SO_3^-	IdoA	H	H

Fig. 35 Structures of five designed hexasaccharides.

residue that selectively activates heparin cofactor II (HCII). HCII is a serine protease that is known to bind to GAGs, such as heparan sulphate, which mediates its inhibition of thrombin. HCII bears considerable similarity to antithrombin (AT), they are homologous in primary, secondary and tertiary structure. However, Fondaparinux binds specifically to AT and heparin binds non-specifically to HCII. Based on this information, Desai and co-workers synthesized five analogues of heparan sulphate (Fig. 35) to bind to HCII specifically from a computational analysis of a library of analogues. The five heparan sulphate sequences were then tested for activation of AT and HCII, with resultant activities similar to predicted activities (Fig. 36). Analog HX3 induces HCII activation by 250-fold, which is similar to AT activation by fondaparinux. The structure of HX3 contains two consecutive GlcA2S residues, which is rare in natural heparan sulphate. These results highlight the benefits of using computational tools and the potential for future GAG design.

Patel and co-workers[216] investigated the anti-cancer activity of heparan sulphate oligosaccharides of various lengths against cancer stem cells (CSCs). CSCs are a small population of cancer cells that self-renew, invade the matrix, and differentiate to bulk tumors.[217–219] Patel and others discovered that the most

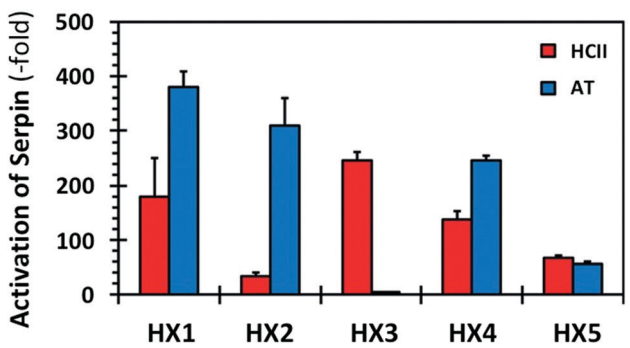

Fig. 36 Comparison of the conformational activation of serpins HCII and AT induced by the CVLS-designed HS hexassacharides. Conformational activation was studied through increase in rate constant of inhibition of either thrombin or factor Xa, the tow primary protease targets of HCII and AT, respectively. Activation of serpin (*y*-axis) refers to the ratio of second order rate constant if inhibition in the presence of HX (k_{HX}) to that in its absence (k_{UNCAT}). Adapted with permission from N. V. Sankaranarayanan, T. R. Strebel, R. S. Boothello, K. Sheerin, A. Raghuraman, F. Sallas, P. D. Mosier, N. D. Watermeyer, S. Oscarson and U. R. Desai, *Angew. Chem.*, 2017, **129**, 2352–2357. Copyright 2017, John Wiley and Sons publishing.

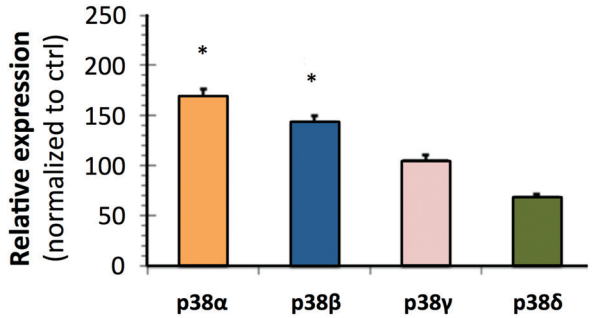

Fig. 37 The corresponding bar graph representation of relative expression shows activation of α and β isoforms, inhibition of δ isoform, and no significant change in γ isoform upon HS06 treatment (100 μM @ 3 h) in HT29 cells. Adapted with permission from N. J. Patel, C. Sharon, S. Baranwal, R. S. Boothello, U. R. Desai and B. B. Patel, *Oncotarget*, 2016, **7**, 84608–84622, under Creative Commons Attribution 3.0 International license, Impact Journals publishing.

common hexasaccharide sequence found in heparan sulphate (HS06) induces selective and specific activation of mitogen-activated protein kinases (MAPK) to inhibit CSCs. Specifically, HS06 selectively inhibits CSCs in an isoform-specific manner by activating p38α and p38β, without activating other MAPK family members as seen in Fig. 37 with a human colon cancer cell line (HT-29).

Mircoarrays

Seeberger and coworkers[220] developed a microarray with synthetic heparin oligosaccharides for detection of heparin–protein interactions. Three heparin oligosaccharides of different lengths were synthesized *via* automated solid phase synthesis[221] from just six monosaccharide building blocks.[222] The oligosaccharides were attached to an amine functionalized thiol linker (Fig. 38) and covalently bound to an amine-reactive CodeLink glass slide (*i.e.*, contains *N*-hydroxysuccinimide esters). The microarrays were incubated with fibroblast growth factor 1 (FGF-1) or FGF-2, followed by anti-human FGF polyclonal antibodies. Visualization of the FGF captured by the array was achieved with a secondary antibody labelled with an Alexa 546 dye (Fig. 39). Oligosaccharides **47** and **48** bound FGF-1 and FGF-2 the best, but interestingly one monosaccharide exhibited a spot intensity for FGF-1 comparable to that of the longer oligosaccharides. This method is being used to identify other heparin–protein interactions.

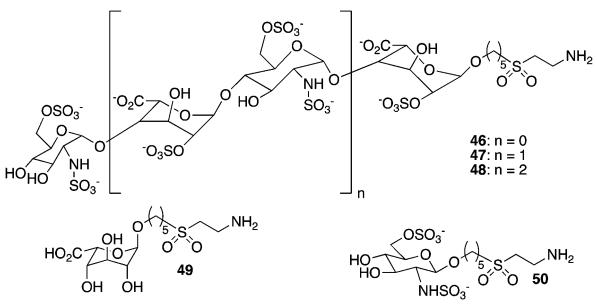

Fig. 38 Heparin oligosaccharides **46**, **47**, and **48** and monosaccharide controls **49** and **50** ready for immobilization on a chip surface.

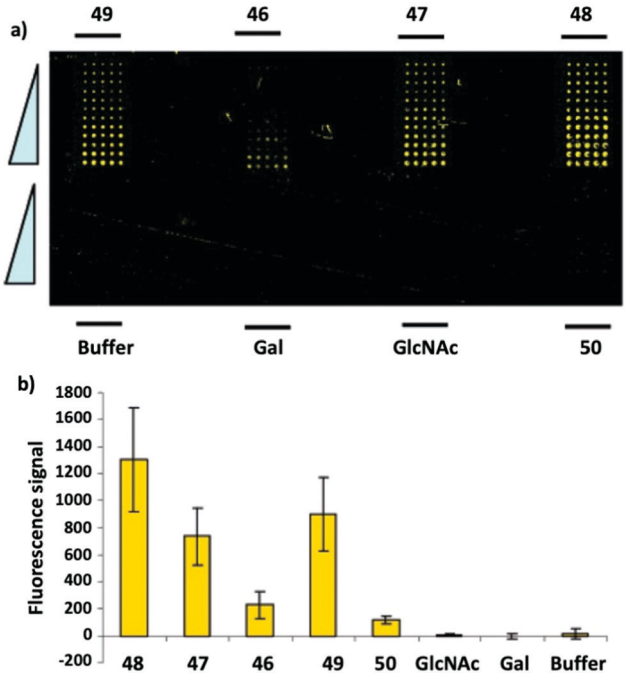

Fig. 39 (a) Microarray after incubation with FGF-1. (b) Fluorescence signal observed for each arrayed carbohydrate binding to FGF-1 at 500 μM. Sodium phosphate buffer served as a negative control. Adapted with permission from J. L. de Paz, C. Noti and P. H. Seeberger, *J. Am. Chem. Soc.*, 2006, **128**, 2766–2767. Copyright 2006, American Chemical Society publishing.

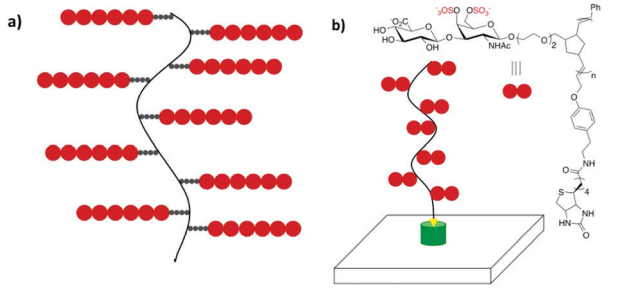

Fig. 40 (a) Schematic representation of a proteoglycan, which typically consists of multiple GAG chains attached to a protein core. (b) Biotin end-functionalized ROMP polymers as mimetics of CS proteoglycans, n = ~80–280. Adapted from S. G. Lee, J. M. Brown, C. J. Rogers, J. B. Matson, C. Krishnamurthy, M. Rawat and L. C. Hsieh-Wilson, *Chem. Sci.*, 2010, **1**, 322–325, with permission from the Royal Society of Chemistry.

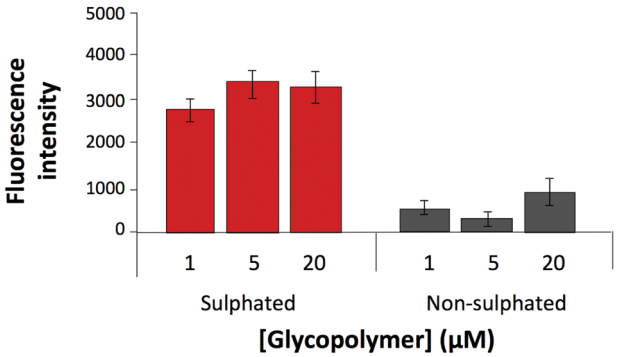

Fig. 41 Binding of GDNF to sulphated and non-sulphated glycopolymers. Adapted from S. G. Lee, J. M. Brown, C. J. Rogers, J. B. Matson, C. Krishnamurthy, M. Rawat and L. C. Hsieh-Wilson, *Chem. Sci.*, 2010, **1**, 322–325, with permission from the Royal Society of Chemistry.

Lee and Brown[223] explored the multivalent architecture of GAGs *via* synthesis of end-functionalized GAG mimetic glycopolymers. A norbornene-based backbone was chosen as to use a ring-opening metathesis polymerization (ROMP) for synthesis of the glycopolymer. Pendant sugar chains were sulphated before polymerization with sulphur trioxide trimethyl amine in DMF at 50 °C (83% yield). The ROMP reaction proceeded quickly in a 1 : 5 co-solvent of MeOH and $(CH_2Cl)_2$ with 1.0% Grubbs catalyst $(H_2IMes)(Py)_2(Cl)_2$ RuCHPh with complete conversion in five minutes to the desired glycopolymer (Fig. 40). Decreasing the catalyst loading to 0.5% gave longer chain lengths (DP = 281; PDI = 1.07).

The glycopolymer mimetics were end-functionalized with a biotin moiety to examine interactions with proteins by attaching them to microarray surfaces. The monoclonal anti-bodies 2D11 and 2D5, which are selective for chondroitin sulphate binding, were evaluated against these GAG mimetics. Antibody 2D11 selectively bound to the sulphated glycopolymer, but not the non-sulphated one. The sulphated glycopolymer also bound to the growth factor, glial cell-derived neurotropic factor (GDNF), which is responsible for the survival and differentiation of dopaminergic neurons (Fig. 41).[12,13] These studies demonstrate that glycopolymer mimetics can be attached to surfaces and bind proteins.

Lung disorders

Taniguchi and co-workers[224] investigated the activity of a keratan sulphate disaccharide, isolated from the keratanase II digest of shark fin (Gal(6-SO_3)-GlcNAc(6-SO_3) (L4)),[225] against inflammation and the progression of emphysema, a component of chronic obstructive pulmonary disease (COPD). Emphysema arises due to damage of the lung air sacs resulting in breathlessness. In a porcine pancreatic elastase (PPE) induced emphysema mouse model, the keratan sulphate disaccharide reduces the production of inflammatory cells, neutrophils and macrophages, and inflammatory cytokines (IL-6 and TNF-α) in the bronchoalveolar lavage fluid. Therefore it is thought to block both immune cell migration and subsequent inflammation in the lung. Inflammation is one of the important factors that triggers the onset and/or progression of COPD,[226] and a better understanding of the role of lung GAGs is important for development of novel therapeutics. Taniguchi previously discovered that this keratan sulphate disaccharide has inhibitory activity on flagellin-induced IL-8 production,[227] a known attractant for inflammatory cells. Overall, the keratan sulphate disaccharide attenuates emphysema *via* its multiple anti-inflammatory activities.

Desai and co-workers[228] studied the high neutrophil elastase (NE) activity of heparin oligosaccharides in the lung and sputum of cystic fibrosis (CF) patients. CF is a multifactorial disease where the protease–antiprotease balance plays an important role. Currently the therapy options for CF patients do not include an

approved drug to inhibit neutrophil serine proteases (NSPs), which play a significant role in airway injury. Re-establishment of the protease–antiprotease balance through inhibition of NE is an attractive pathway for lung injury prevention. To investigate this, Desai utilized 2-*O*,3-*O*-desulphated heparin (ODSH), to target heparin's anti-inflammatory and antiprotease activity with minimal anti-coagulant activity as an anti-NE agent in CF.[229,230] In comparison to three DNA variants (6-, 12- and 24-mer), ODSH displayed more potent NE-activity *in vitro*. The anti-NE activity of ODSH and DNA was chain length dependant to give effective inhibition. DNA chains of 6-mer or shorter did not inhibit NE. Likewise ODSH chains of 15-mer or shorter did not inhibit NE.

It is known that NE increases high mobility group box 1 (HMGB1) release *in vivo*, which activates the receptor for advanced glycation end (RAGE), increasing inflammation and mucin.[231] HMGB1 is released from macrophages after inflammation and is a biomarker in CF patients of lung disease progression. Voynow and co-workers[232] report that ODSH inhibits HMBG1 release from murine macrophages, both *in vivo* and *in vitro via* inhibition of a histone acetyltranferase, p300. Acetylation of HMGB1 is required for secretion.[233] ODSH inhibits both NE- and LPS-mediated HMGB1 release in a concentration dependant manner. Additionally, ODSH specifically inhibits HAT-catalysed lysine acetylation of HMGB1 in a dose dependant manner. Finally they investigated whether p300 was a specific HAT target for ODSH (Fig. 42A) and discovered that ODSH inhibits p300 activity and p300-catalysed HMGB1 acetylation in a concentration dependant manner (Fig. 42B). Overall, there is potential for heparin-based anti-inflammatory drugs for NE protease, p300, and HMGB1 inhibition in CF.

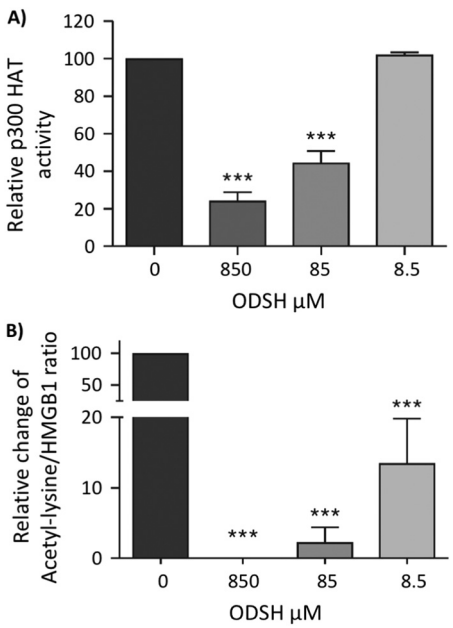

Fig. 42 ODSH inhibited p300 histone acetyltransferase (HAT) activity and p300-induced HMGB1 acetylation *in vitro* in a concentration-dependant manner. (A) ODSH 85 and 850 μM significantly inhibited p300 HAT activity ($P < 0.001$). (B) All ODSH treatments significantly decreased acetyllysine/HMGB1 level compared with no ODSH treatment ($P < 0.001$). Adapted from S. Zheng, A. B. Kummarapurugu, D. K. Afosah, N. V. Sankaranarayanan, R. S. Boothello, U. R. Desai, T. Kennedy and J. A. Voynow, *Am. J. Respir. Cell Mol. Biol.*, 2017, **56**, 90–98 with permission from American Thoraic Society Journals.

Kerns and co-workers[234] synthesized a small library of *N*-arylacyl *O*-sulphonated aminoglycosides as mimetics of LMWH and tested their activity against three neutrophil serine proteases (NSPs): human neutrophil elastase (HNE), cathepsin G (CatG) and proteinase 3 (Pr3). The glycosides were tri- or tetrasacharides with neomycin (Neo), kanamycin (Kan) or apramycin (Apr) as the core and benzoyl (Bz), phenylacetyl (PhA) and carbobenzyloxy (Cbz) as the aryl groups with sulphates at the hydroxyls (Fig. 43). Each compound was screened for inhibition of each NSP *via* a peptide cleavage assay. The IC_{50} values are summarized in Table 4, with NeoCbz being the most potent inhibitor for HNE (IC_{50} = 8.13 μM), and CatG (IC_{50} = 0.42 μM), while KanCbz (IC_{50} = 16.98 μM) moderately inhibits Pr3. In general the neomycin and kanamycin derivatives are more potent inhibitors indicating that a more flexible core increases their activity by allowing for better

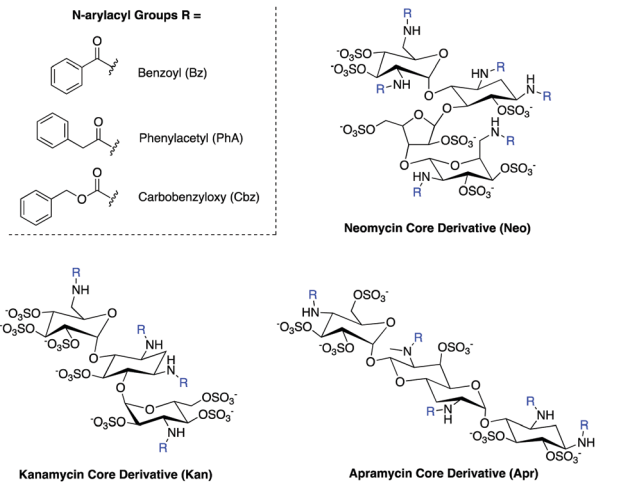

Fig. 43 Structures of *N*-arylacyl *O*-sulphonated aminoglycosides. Neomycin, kanamycin and apramycin are *N*-substituted with three different arylacyl groups and per-*O*-sulphonated, affording nine derivatives.

Table 4 Half-maximal inhibitory concentration of *N*-arylacyl *O*-sulphonated aminoglycosides for inhibition of each NSP

Compound	Human neutrophil elastase,[a] IC_{50} (μM)	Cathepsin G,[b] IC_{50} (μM)	Proteinase 3,[a] IC_{50} (μM)
NeoCbz	8.13 ± 3.39	0.42 ± 0.03	>300
NeoPhA	>300	1.29 ± 0.21	97.72 ± 22.75
NeoBz	>300	1.55 ± 0.36	>300
KanCbz	16.60 ± 7.55	3.72 ± 0.17	16.98 ± 5.18*
KanPhA	229.09 ± 58.99	12.3 ± 1.42	165.96 ± 58.75
KanBz	>300	26.92 ± 5.63	>300
AprCbz	20.42 ± 11.45	2.14 ± 0.2	26.92 ± 18.52
AprPhA	263.03 ± 30.37	123.03 ± 11.35	NI
AprBz	NI	208.93 ± 24.68	ND

NI, no inhibition; ND, not determined. IC_{50} values derived from non-linear regression curve fitting to log (inhibitor) *vs.* normalized response. Data are shown as mean ± SE (n = 3 or *n = 2). [a] Substrates: *N*-methoxysuccinyl-Ala-Ala-Pro_Val-*p*-nitroanilide. [b] *N*-Succinyl-Ala-Ala-Pro-Phe-*p*-nitroanilide.

binding to the proteases. KanCbz possesses the greatest inhibition over all three of the NSPs, while NeoCbz is a potent dual inhibitor of HNE and CatG. This study demonstrates that *N*-arylacetyl *O*-sulphonated aminoglycosides can be further explored as lead structures for novel, multi-target NSP inhibitor drugs for attenuating protease-mediated inflammatory lung diseases.

Conclusions

Compositionally and structurally, sulphated polysaccharides are and continue to be of substantial interest given their diverse biological activities. A wide variety of sulphation reagents are described in the literature and are used to varying degrees of success in terms of yield, reactivity, regioselectivity, and scope. The most common and reliable method today employs sulphur trioxide–pyridine complexes, and we recommend this reagent as a starting point in a polysaccharide sulphation reaction. Recent alternative methods include microwave reactions, utilization of DMAP as a catalyst to decrease the reaction time, sulphate protecting groups to mask the anionic character of the sulphate, and chemoenzymatic reactions. Of the characterization methods utilized, elemental analysis along with NMR and IR spectroscopy are widely used to estimate the degree of sulphation and to determine site of sulphation. From a chemical perspective, significant opportunities exist for improvement including: (1) higher sulphation reaction yields; (2) better sulphation regioselectivity compared to the current methods which utilize sugar protecting group strategies to mask the other hydroxyl groups; (3) sulphate protecting groups stable to both nucleophilic and acid/base conditions; (4) methods to install the sulphate group while synthesizing a polysaccharide instead of post-polymerization transformations; (5) further computational studies on sulphated polysaccharides using the most recent atomistic force fields (GROMOS, CHARMM and GLYCAM); and (6) expanded computational studies of polysaccharide–protein interactions beyond the current heparin and GAG mimetic studies.

The first clinical use of a well-defined sulphated polysaccharide – heparin – was achieved in 1935, almost two decades following its discovery in 1916. To the best of our knowledge no other sulphated natural polysaccharide is FDA (or other governmental agency) approved and used in the clinic. Of the sulphated synthetic polysaccharides, Fondaparinux is the only marketed product. This short list of successful commercial products is focused on anticoagulation activity. Thus, from an application perspective, extensive opportunities exist to: (1) develop and translate either naturally or chemically sulphated natural polysaccharides with antiviral or anticancer bioactivities; (2) investigate synthetic polysaccharides as a carrier and/or targeting moiety for drug delivery; and (3) incorporate synthetic sulphated polysaccharides into biomaterials, such as nanoparticles or nanogels. There are several examples of polysaccharide-based nanoparticles with naturally sulphated polysaccharides[235,236] as drug delivery systems.[235] However, there are few groups developing drug delivery systems with synthetic sulphated polysaccharides, both sulphated natural polysaccharides[237] or fully synthetic sulphated polysaccharides.[238,239]

In recent years, advances in the synthesis and characterization of sulphated polysaccharides are increasingly enabling rigorous evaluation of their biocompatibility and potential use as therapeutics. These studies are providing insights into structure–activity relationships as well as guidance on identifying the specific structural components or functional groups critical to bioactivity. The full potential of sulphated polysaccharides as active agents for antioxidation, anticancer, antiviral, anti-inflammation biomedical applications is significant, and we are only at the beginning. We see the next ten years to be exciting times filled with new discoveries, research, innovation, and translation. We encourage all to investigate and contribute to this area, which is at the intersection of the chemistry, engineering, and medicine disciplines.

Conflicts of interest

There are no conflicts to declare.

Acknowledgements

This work was supported in part by BU, L'Oréal, and DOD USU (HU0001810012). Discussions with Dr. Magali Moreau at the Advanced Research L'Oréal Center in New Jersey are greatly appreciated.

References

1 L. Zhao, M. Wu, C. Xiao, L. Yang, L. Zhou, N. Gao, Z. Li, J. Chen, J. Chen, J. Liu, H. Qin and J. Zhao, *Proc. Natl. Acad. Sci. U. S. A.*, 2015, **112**, 8284–8289.
2 G. Jiao, G. Yu, J. Zhang and H. S. Ewart, *Mar. Drugs*, 2011, **9**, 196–223.
3 M. Gama, H. B. Nader and H. A. Rocha, *Sulfated Polysaccharides (Biochemistry and Molecular Biology in the Post Genomic Era)*, Nova Science Pub Inc., 2015.
4 R. C. R. Oliveira, R. R. Almeida and T. A. Goncalves, *J. Dev. Drugs*, 2016, **5**, 166–168.
5 J. Necas and L. Bartosikova, *Vet. Med.*, 2013, **58**, 187–205.
6 Z. J. Wang, J. H. Xie, M. Y. Shen, S. P. Nie and M. Y. Xie, *Trends Food Sci. Technol.*, 2018, **74**, 147–157.
7 T. Zaporozhets and N. Besednova, *Pharm. Biol.*, 2016, **54**, 3126–3135.
8 M. F. Raposo, R. M. de Morais and A. M. Bernardo de Morais, *Mar. Drugs*, 2013, **11**, 233–252.
9 L. Cunha and A. Grenha, *Mar. Drugs*, 2016, **14**, 42–82.
10 D. C. Sun, *Ann. N. Y. Acad. Sci.*, 1967, **140**, 747–761.
11 R. G. Bianchi and D. L. Cook, *Gastroenterology*, 1964, **47**, 409–414.
12 L. F. Lin, D. H. Doherty, J. D. Lile, S. Bektesh and F. Collins, *Science*, 1993, **260**, 1130–1132.
13 A. Tomac, E. Lindqvist, L. F. Lin, S. O. Ogren, D. Young, B. J. Hoffer and L. Olson, *Nature*, 1995, **373**, 335–339.

14 B. Kaeffer, C. Benard, M. Lahaye, H. M. Blottiere and C. Cherbut, *Planta Med.*, 1999, **65**, 527–531.
15 M. W. Piepkorn, G. Schmer and D. Lagunoff, *Thromb. Res.*, 1978, **13**, 1077–1087.
16 R. C. Appleyard, D. Burkhardt, P. Ghosh, R. Read, M. Cake, M. V. Swain and G. A. Murrell, *Osteoarthr. Cartil.*, 2003, **11**, 65–77.
17 M. J. Osborn, S. M. Rosen, L. Rothfield, L. D. Zeleznick and B. L. Horecker, *Science*, 1964, **145**, 783–789.
18 S. U. Hansen, G. J. Miller, M. J. Cliff, G. C. Jayson and J. M. Gardiner, *Chem. Sci.*, 2015, **6**, 6158–6164.
19 J. A. Singh, S. Noorbaloochi, R. MacDonald and L. J. Maxwell, *Cochrane Database Sys. Rev.*, 2015, **1**, CD005614.
20 J. B. Lee, T. Hayashi, K. Hayashi and U. Sankawa, *J. Nat. Prod.*, 2000, **63**, 136–138.
21 K. Hayashi, T. Hayashi and I. Kojima, *AIDS Res. Hum. Retroviruses*, 1996, **12**, 1463–1471.
22 A. Kausar, S. Zulfiqar and M. I. Sarwar, *Polym. Rev.*, 2014, **54**, 185–267.
23 J. J. Griebel, R. S. Glass, K. Char and J. Pyun, *Prog. Polym. Sci.*, 2016, **58**, 90–125.
24 J. L. Funderburgh, *Glycobiology*, 2000, **10**, 951–958.
25 B. Li, F. Lu, X. Wei and R. Zhao, *Molecules*, 2008, **13**, 1671–1695.
26 R. A. Al-Horani and U. R. Desai, *Tetrahedron*, 2010, **66**, 2907–2918.
27 C. L. Zhou, W. Liu, Q. Kong, Y. Song, Y. Y. Ni, Q. H. Li and D. O'Riordan, *Int. J. Food Sci. Technol.*, 2014, **49**, 508–514.
28 J. M. Trowbridge and R. L. Gallo, *Glycobiology*, 2002, **12**, 117R–125R.
29 A. Richter and D. Klemm, *Cellulose*, 2003, **10**, 133–138.
30 A. Raghuraman, M. Riaz, M. Hindle and U. R. Desai, *Tetrahedron Lett.*, 2007, **48**, 6754–6758.
31 C. O. Kappe and D. Dallinger, *Nat. Rev. Drug Discovery*, 2006, **5**, 51–63.
32 S. F. Yakuoka, S. Yamaguchi, T. Sakurai and K. Okuyama, *J. Biochem.*, 1973, **74**, 425–434.
33 T. Yoshida, Y. Yasuda, T. Mimura, Y. Kaneko, H. Nakashima, N. Yamamoto and T. Uryu, *Carbohydr. Res.*, 1995, **276**, 425–436.
34 C. Mahner, M. D. Lechner and E. Nordmeier, *Carbohydr. Res.*, 2001, **331**, 203–208.
35 X. Huang and W. D. Zhang, *JFBI*, 2010, **3**, 32–39.
36 V. A. Levdansky, A. S. Kondracenko, A. V. Levdansky, B. N. Kuznetsov, L. Djakovitch and C. Pinel, *J. Sib. Fed. Univ., Chem.*, 2014, **7**, 162–169.
37 X. Si, Z. Zhou, D. Bu, J. Li, P. Strappe and C. Blanchard, *CyTA–J. Food*, 2016, 1–10, DOI: 10.1080/19476337.2016.1176074.
38 I. Yamamoto, K. Takayama, T. Gonda, K. Matsuzaki, K. Hatanaka, T. Yoshida, T. Uryu, O. Yoshida, H. Nakashima, N. Yamamoto, Y. Kaneko and T. Mimura, *Br. Polym. J.*, 1990, **23**, 245–250.
39 K. Nagasawa, H. Harada, S. Hayashi and T. Misawa, *Carbohydr. Res.*, 1972, **21**, 420–426.
40 K. Hatanaka, T. Hirobe, T. Yoshida, M. Yamanaka and T. Uyru, *Polym. J.*, 1990, **22**, 435–441.
41 K. Nagasawa and H. Yoshidome, *Chem. Pharm. Bull.*, 1969, **17**, 1316–1323.
42 G. Vikhoreva, G. Bannikova, P. Stolbushkina, A. Panov, N. Drozd, V. Makarov, V. Varlamov and L. Gal'braikh, *Carbohydr. Polym.*, 2005, **62**, 327–332.
43 J. Wang, W. Yang, T. Yang, X. Zhang, Y. Zuo, J. Tian, J. Yao, J. Zhang and Z. Lei, *Int. J. Biol. Macromol.*, 2015, **74**, 61–67.
44 D. J. Berry, C. V. Digiovanna, S. S. Metrick and R. Murugan, *ARKIVOC*, 2005, **2001**, 201–226.
45 S. Yoda, D. Bratton and S. M. Howdle, *Polymer*, 2004, **45**, 7839–7843.
46 T. Chen, B. Li, Y. Li, C. D. Zhao, J. M. Shen and H. X. Zhang, *Carbohydr. Polym.*, 2011, **83**, 554–560.
47 X. Liu, T. Chen, Y. Hu, K. Li and L. Yan, *Biopolymers*, 2014, **101**, 210–215.
48 J. Wang, S. Niu, B. Zhao, T. Luo, D. Liu and J. Zhang, *Carbohydr. Polym.*, 2014, **107**, 221–231.
49 C. L. Penney and A. S. Perlin, *Carbohydr. Res.*, 1981, **93**, 241–246.
50 A. D. Proud, J. C. Prodger and S. L. Flitsch, *Tetrahedron Lett.*, 1997, **38**, 7243–7246.
51 L. J. Ingram and S. D. Taylor, *Angew. Chem., Int. Ed.*, 2006, **45**, 3503–3506.
52 L. J. Ingram, A. Desoky, A. M. Ali and S. D. Taylor, *J. Org. Chem.*, 2009, **74**, 6479–6485.
53 R. W. Binkley and D. G. Hehemann, *J. Org. Chem.*, 1990, **55**, 378–380.
54 A. Y. Desoky and S. D. Taylor, *J. Org. Chem.*, 2009, **74**, 9406–9412.
55 L. S. Simpson and T. S. Widlanski, *J. Am. Chem. Soc.*, 2006, **128**, 1605–1610.
56 J. C. Roberts, H. Gao, A. Gopalsamy, A. Kongsjahju and R. J. Patch, *Tetrahedron Lett.*, 1997, **38**, 355–358.
57 M. Q. Xie and T. S. Widlanski, *Tetrahedron Lett.*, 1996, **37**, 4443–4446.
58 E. Buncel, *Chem. Rev.*, 1970, **70**, 323–337.
59 Y. Xu, K. Chandarajoti, X. Zhang, V. Pagadala, W. Dou, D. M. Hoppensteadt, E. M. Sparkenbaugh, B. Cooley, S. Daily, N. S. Key, D. Severynse-Stevens, J. Fareed, R. J. Linhardt, R. Pawlinski and J. Liu, *Sci. Transl. Med.*, 2017, **9**, eaan5954.
60 Y. Xu, C. Cai, K. Chandarajoti, P. H. Hsieh, L. Li, T. Q. Pham, E. M. Sparkenbaugh, J. Sheng, N. S. Key, R. Pawlinski, E. N. Harris, R. J. Linhardt and J. Liu, *Nat. Chem. Biol.*, 2014, **10**, 248–250.
61 Y. Xu, S. Masuko, M. Takieddin, H. Xu, R. Liu, J. Jing, S. A. Mousa, R. J. Linhardt and J. Liu, *Science*, 2011, **334**, 498–501.
62 W. Lu, C. Zong, P. Chopra, L. E. Pepi, Y. Xu, I. J. Amster, J. Liu and G. J. Boons, *Angew. Chem., Int. Ed.*, 2018, **57**, 5340–5344.
63 D. A. Hall, *Biochem. J.*, 1955, **59**, 459–465.
64 J. I. Gross, M. B. Mathews and A. Dorfman, *J. Biol. Chem.*, 1960, **235**, 2889–2892.
65 J. Polatnick, A. J. La Tessa and H. M. Katzin, *Biochim. Biophys. Acta*, 1957, **26**, 361–364.
66 K. S. Dodgson and R. G. Price, *Biochem. J.*, 1962, **84**, 106–110.

67 Y. Lijour, E. Gentric, E. Deslandes and J. Guezennec, *Anal. Biochem.*, 1994, **220**, 244–248.
68 H. Korva, J. Karkkainen, K. Lappalainen and M. Lajunen, *Starch-Stärke*, 2016, **68**, 854–863.
69 M. W. Kačuráková and R. H. Wilson, *Carbohydr. Polym.*, 2001, **44**, 291–303.
70 E. K. Kemsley, Z. Li, M. K. Hammouri and R. H. Wilson, *Food Chem.*, 1992, **44**, 299–304.
71 V. M. Doctor and D. Esho, *Carbohydr. Res.*, 1983, **121**, 312–315.
72 S. Alban, A. Schauerte and G. Franz, *Carbohydr. Polym.*, 2002, **47**, 267–276.
73 P. K. Smith, A. K. Mallia and G. T. Hermanson, *Anal. Biochem.*, 1980, **109**, 466–473.
74 F. C. MacIntosh, *Biochem. J.*, 1941, **35**, 776–782.
75 A. L. Copley and D. V. Whitney III, *J. Lab. Clin. Med.*, 1943, **28**, 7620770.
76 U. Warttinger, C. Giese and R. Kramer, *Comparison of Heparin Red, Azure A and Toluidine Blue assays for direct quantification of heparins in human plasma*, 2017.
77 C. A. Antonopoulos, A. F. Daniel, R. Havanka, T. Briggs, G. A. D. Haslewood and H. Flood, *Acta Chem. Scand.*, 1962, **16**, 1521–1522.
78 M. A. Tabatabai, *Environ. Lett.*, 1974, **7**, 237–243.
79 C. Deng, J. Xu, H. Fu, J. Chen and X. Xu, *Mol. Med. Rep.*, 2015, **11**, 2991–2998.
80 M. Remko and C. W. von der Lieth, *J. Chem. Inf. Model.*, 2006, **46**, 1687–1694.
81 M. Remko and C. W. von der Lieth, *J. Phys. Chem. A*, 2007, **111**, 13484–13491.
82 M. Remko, P. T. Van Duijnen and R. Broer, *RSC Adv.*, 2013, **3**, 9843–9853.
83 N. S. Gandhi and R. L. Mancera, *Carbohydr. Res.*, 2010, **345**, 689–695.
84 S. S. Mallajosyula, O. Guvench, E. Hatcher and A. D. Mackerell Jr., *J. Chem. Theory Comput.*, 2012, **8**, 759–776.
85 R. D. Lins and P. H. Hunenberger, *J. Comput. Chem.*, 2005, **26**, 1400–1412.
86 C. Oostenbrink, A. Villa, A. E. Mark and W. F. van Gunsteren, *J. Comput. Chem.*, 2004, **25**, 1656–1676.
87 H. Yu, M. Amann, T. Hansson, J. Kohler, G. Wich and W. F. van Gunsteren, *Carbohydr. Res.*, 2004, **339**, 1697–1709.
88 L. Pol-Fachin, V. H. Rusu, H. Verli and R. D. Lins, *J. Chem. Theory Comput.*, 2012, **8**, 4681–4690.
89 K. N. Kirschner, A. B. Yongye, S. M. Tschampel, J. Gonzalez-Outeirino, C. R. Daniels, B. L. Foley and R. J. Woods, *J. Comput. Chem.*, 2008, **29**, 622–655.
90 M. Basma, S. Sundara, D. Calgan, T. Vernali and R. J. Woods, *J. Comput. Chem.*, 2001, **22**, 1125–1137.
91 A. Singh, M. B. Tessier, K. Pederson, X. Wang, A. P. Venot, G. J. Boons, J. H. Prestegard and R. J. Woods, *Can. J. Chem.*, 2016, **94**, 927–935.
92 B. Nagarajan, N. V. Sankaranarayanan and U. R. Desai, *Wiley Interdiscip. Rev.: Comput. Mol. Sci.*, 2018, DOI: 10.1002/wcms.1388.
93 A. Almond, *Curr. Opin. Struct. Biol.*, 2018, **50**, 58–64.
94 N. V. Sankaranarayanan, B. Nagarajan and U. R. Desai, *Curr. Opin. Struct. Biol.*, 2018, **50**, 91–100.
95 I. Capila and R. J. Linhardt, *Angew. Chem., Int. Ed.*, 2002, **41**, 390–412.
96 U. Lindahl, K. Lidholt, D. Spillman and L. Kjellén, *Thromb. Res.*, 1994, **75**, 1–32.
97 D. R. Coombe and W. C. Kett, *Handb. Exp. Pharmacol.*, 2012, 361–383, DOI: 10.1007/978-3-642-23056-1_16.
98 S. M. Bromfield, E. Wilde and D. K. Smith, *Chem. Soc. Rev.*, 2013, **42**, 9184–9195.
99 E. I. Oduah, R. J. Linhardt and S. T. Sharfstein, *Pharmaceuticals*, 2016, **9**, 38–49.
100 I. Ahmed, A. Majeed and R. Powell, *Postgrad. Med. J.*, 2007, **83**, 575–582.
101 J. McLean, *Circulation*, 1959, **19**, 75–78.
102 R. L. Bick, E. P. Frenkel, J. Walenga, J. Fareed and D. A. Hoppensteadt, *Hematol./Oncol. Clin. North Am.*, 2005, **19**, 1–51, v.
103 K. Chandarajoti, J. Liu and R. Pawlinski, *J. Thromb. Haemostasis*, 2016, **14**, 1135–1145.
104 J. Silvain, F. Beygui, O. Barthelemy, C. Pollack Jr., M. Cohen, U. Zeymer, K. Huber, P. Goldstein, G. Cayla, J. P. Collet, E. Vicaut and G. Montalescot, *Br. Med. J.*, 2012, **344**, e553.
105 D. Park, W. Southern, M. Calvo, M. Kushnir, C. Solorzano, M. Sinnet and H. H. Billett, *J. Gen. Intern. Med.*, 2016, **31**, 182–187.
106 M. J. Martinez-Zapata, A. G. Mathioudakis, S. A. Mousa and R. Bauersachs, *Clin. Appl. Thromb./Hemostasis*, 2018, **24**, 226–234.
107 E. Ersdal-Badju, A. Lu, Y. Zuo, V. Picard and S. C. Bock, *J. Biol. Chem.*, 1997, **272**, 19393–19400.
108 L. Jin, J. P. Abrahams, R. Skinner, M. Petitou, R. N. Pike and R. W. Carrell, *Proc. Natl. Acad. Sci. U. S. A.*, 1997, **94**, 14683–14688.
109 D. J. Johnson, W. Li, T. E. Adams and J. A. Huntington, *EMBO J.*, 2006, **25**, 2029–2037.
110 W. Li, D. J. Johnson, C. T. Esmon and J. A. Huntington, *Nat. Struct. Mol. Biol.*, 2004, **11**, 857–862.
111 Z. Cai, S. V. Yarovoi, Z. Zhu, L. Rauova, V. Hayes, T. Lebedeva, Q. Liu, M. Poncz, G. Arepally, D. B. Cines and M. I. Greene, *Nat. Commun.*, 2015, **6**, 8277.
112 N. M. Mestechkina and V. D. Shcherbukhin, *Appl. Biochem. Microbiol.*, 2010, **46**, 267–273.
113 C. A. de Araujo, M. D. Noseda, T. R. Cipriani, A. G. Goncalves, M. E. Duarte and D. R. Ducatti, *Carbohydr. Polym.*, 2013, **91**, 483–491.
114 A. Chaidedgumjorn, H. Toyoda, E. R. Woo, K. B. Lee, Y. S. Kim, T. Toida and T. Imanari, *Carbohydr. Res.*, 2002, **337**, 925–933.
115 A. Golas, C. H. Yeh, C. A. Siedlecki and E. A. Vogler, *Biomaterials*, 2011, **32**, 9747–9757.
116 J. Yang, Y. Du, R. Huang, Y. Wan and Y. Wen, *Int. J. Biol. Macromol.*, 2005, **36**, 9–15.
117 J. H. Yang, Y. M. Du, Y. Wen, T. Y. Li and L. Hu, *Carbohydr. Polym.*, 2003, **52**, 397–403.

118 J. Yang, Y. Du, R. Huang, Y. Wan and T. Li, *Int. J. Biol. Macromol.*, 2002, **31**, 55–62.
119 S. Alban, W. Jeske, D. Welzel, G. Franz and J. Fareed, *Thromb. Res.*, 1995, **78**, 201–210.
120 A. N. O'Neill, *Can. J. Chem.*, 1955, **33**, 1097–1101.
121 T. Muschin, D. Budragchaa, T. Kanamoto, H. Nakashima, K. Ichiyama, N. Yamamoto, H. Shuqin and T. Yoshida, *Int. J. Biol. Macromol.*, 2016, **89**, 415–420.
122 Y. Roman, H. P. de Oliveira Barddal, M. Iacomini, G. L. Sassaki and T. R. Cipriani, *Carbohydr. Polym.*, 2017, **174**, 731–739.
123 Y. L. Zhang, J. B. Zhang, X. Y. Mo, X. Y. Lu, Y. N. Zhang and L. G. Qin, *Carbohydr. Polym.*, 2010, **82**, 515–520.
124 L. Liang, L. Ao, T. Ma, Y. Ni, X. Liao, X. Hu and Y. Song, *Int. J. Biol. Macromol.*, 2018, **106**, 447–455.
125 C. B. S. Telles, D. A. Sabry, J. Almeida-Lima, M. S. S. P. Costa, R. F. Melo-Silveira, E. S. Trindade, G. L. Sassaki, E. Wisbeck, S. A. Furlan, E. L. Leite and H. A. O. Rocha, *Carbohydr. Polym.*, 2011, **85**, 514–521.
126 N. Li, X. Liu, X. He, S. Wang, S. Cao, Z. Xia, H. Xian, L. Qin and W. Mao, *Carbohydr. Polym.*, 2017, **159**, 195–206.
127 A. Magnani, S. Lamponi, R. Rappuoli and R. Barbucci, *Polym. Int.*, 1998, **46**, 225–240.
128 X. Zhang, H. Y. Liu, L. S. Lin, W. Yao, J. H. Zhao, M. Y. Wu and Z. J. Li, *Angew. Chem., Int. Ed.*, 2018, **57**, 12880–12885.
129 M. Guerrini, D. Beccati, Z. Shriver, A. Naggi, K. Viswanathan, A. Bisio, I. Capila, J. C. Lansing, S. Guglieri, B. Fraser, A. Al-Hakim, N. S. Gunay, Z. Zhang, L. Robinson, L. Buhse, M. Nasr, J. Woodcock, R. Langer, G. Venkataraman, R. J. Linhardt, B. Casu, G. Torri and R. Sasisekharan, *Nat. Biotechnol.*, 2008, **26**, 669–675.
130 X. Zhang, V. Pagadala, H. M. Jester, A. M. Lim, T. Q. Pham, A. M. P. Goulas, J. Liu and R. J. Linhardt, *Chem. Sci.*, 2017, **8**, 7932–7940.
131 A. H. Gracher, A. G. Santana, T. R. Cipriani and M. Iacomini, *Carbohydr. Polym.*, 2016, **136**, 177–186.
132 K. Chatterjee, Z. Guo, E. A. Vogler and C. A. Siedlecki, *J. Biomed. Mater. Res., Part A*, 2009, **90**, 27–34.
133 R. J. Fonseca, S. N. Oliveira, F. R. Melo, M. G. Pereira, N. M. Benevides and P. A. Mourao, *Thromb. Haemostasis*, 2008, **99**, 539–545.
134 M. A. Tabatabai and J. M. Bremner, *Soil Sci. Soc. Am. J.*, 1970, **34**, 225–229.
135 C. Zou, Y. Du, Y. Li, J. Yang and L. Zhang, *Int. J. Biol. Macromol.*, 2010, **46**, 140–144.
136 M. C. Rocha de Souza, C. T. Marques, C. M. Guerra Dore, F. R. Ferreira da Silva, H. A. Oliveira Rocha and E. L. Leite, *J. Appl. Phycol.*, 2007, **19**, 153–160.
137 J. L. Wang, H. Y. Guo, J. Zhang, X. F. Wang, B. T. Zhao, J. A. Yao and Y. P. Wang, *Carbohydr. Polym.*, 2010, **81**, 897–905.
138 Y. Xu, S. Song, Y. Wei, F. Wang, M. Zhao, J. Guo and J. Zhang, *Int. J. Biol. Macromol.*, 2016, **87**, 180–190.
139 J. H. Xie, Z. J. Wang, M. Y. Shen, S. P. Nie, B. Gong, H. S. Li, Q. Zhao, W. J. Li and M. Y. Xie, *Food Hydrocolloids*, 2016, **53**, 7–15.
140 J. Li, Z. Chi, L. Yu, F. Jiang and C. Liu, *Int. J. Biol. Macromol.*, 2017, **105**, 1544–1553.
141 Y. Wang, L. Zhang, Y. Li, X. Hou and F. Zeng, *Carbohydr. Res.*, 2004, **339**, 2567–2574.
142 S. Arafuka, N. Koshiba, D. Takahashi and K. Toshima, *Chem. Commun.*, 2014, **50**, 9831–9834.
143 J. Murata, I. Saiki, S. Nishimura, N. Nishi, S. Tokura and I. Azuma, *Jpn. J. Cancer Res.*, 1989, **80**, 866–872.
144 R. Zheng, S. Jie, D. Hanchuan and W. Moucheng, *Int. Immunopharmacol.*, 2005, **5**, 811–820.
145 S. P. Wasser, *Appl. Microbiol. Biotechnol.*, 2002, **60**, 258–274.
146 L. Wang, X. Li and Z. Chen, *Int. J. Biol. Macromol.*, 2009, **44**, 211–214.
147 Z. Sun, Y. He, Z. Liang, W. Zhou and T. Niu, *Carbohydr. Polym.*, 2009, **77**, 628–633.
148 C. R. Parish, C. Freeman, K. J. Brown, D. J. Francis and W. B. Cowden, *Cancer Res.*, 1999, **59**, 3433–3441.
149 L. Q. Chow, D. L. Gustafson, C. L. O'Bryant, L. Gore, M. Basche, S. N. Holden, M. C. Morrow, S. Grolnic, B. R. Creese, K. L. Roberts, K. Davis, R. Addison and S. G. Eckhardt, *Cancer Chemother. Pharmacol.*, 2008, **63**, 65–74.
150 K. D. Lewis, W. A. Robinson, M. J. Millward, A. Powell, T. J. Price, D. B. Thomson, E. T. Walpole, A. M. Haydon, B. R. Creese, K. L. Roberts, J. R. Zalcberg and R. Gonzalez, *Invest. New Drugs*, 2008, **26**, 89–94.
151 C. J. Liu, P. H. Lee, D. Y. Lin, C. C. Wu, L. B. Jeng, P. W. Lin, K. T. Mok, W. C. Lee, H. Z. Yeh, M. C. Ho, S. S. Yang, C. C. Lee, M. C. Yu, R. H. Hu, C. Y. Peng, K. L. Lai, S. S. Chang and P. J. Chen, *J. Hepatol.*, 2009, **50**, 958–968.
152 B. Y. Liao, Z. Wang, J. Hu, W. F. Liu, Z. Z. Shen, X. Zhang, L. Yu, J. Fan and J. Zhou, *Tumour Biol.*, 2016, **37**, 2987–2998.
153 L. M. Khachigian and C. R. Parish, *Cardiovasc. Drug Rev.*, 2004, **22**, 1–6.
154 G. Gu, G. Wei and Y. Du, *Carbohydr. Res.*, 2004, **339**, 1155–1162.
155 T. Karoli, L. Liu, J. K. Fairweather, E. Hammond, C. P. Li, S. Cochran, K. Bergefall, E. Trybala, R. S. Addison and V. Ferro, *J. Med. Chem.*, 2005, **48**, 8229–8236.
156 V. Ferro, C. Li, B. Wang, K. Fewings, A. R. King, E. Hammond and B. R. Creese, *J. Label. Compd. Radiopharm.*, 2002, **45**, 747–754.
157 J. K. Fairweather, E. Hammond, K. D. Johnstone and V. Ferro, *Bioorg. Med. Chem.*, 2008, **16**, 699–709.
158 R. Namme, T. Mitsugi, H. Takahashi and S. Ikegami, *Tetrahedron Lett.*, 2005, **46**, 3033–3036.
159 S. Valerio, A. Pastore, M. Adinolfi and A. Iadonisi, *J. Org. Chem.*, 2008, **73**, 4496–4503.
160 G. Yu, N. S. Gunay, R. J. Linhardt, T. Toida, J. Fareed, D. A. Hoppensteadt, H. Shadid, V. Ferro, C. Li, K. Fewings, M. C. Palermo and D. Podger, *Eur. J. Med. Chem.*, 2002, **37**, 783–791.
161 K. K. Takemoto and S. S. Spicer, *Ann. N. Y. Acad. Sci.*, 2006, **130**, 365–373.
162 K. A. Yamamoto, L. C. Galhardi, V. P. Rincao, A. Soares Sde, I. G. Vieira, N. M. Ricardo, C. Nozawa and R. E. Linhares, *Int. J. Biol. Macromol.*, 2013, **52**, 9–13.

163 N. Lopes, S. Ray, S. F. Espada, W. A. Bomfim, B. Ray, L. C. Faccin-Galhardi, R. E. C. Linhares and C. Nozawa, *Int. J. Biol. Macromol.*, 2017, **102**, 605–612.
164 S. Saha, M. H. Navid, S. S. Bandyopadhyay, P. Schnitzler and B. Ray, *Carbohydr. Polym.*, 2012, **87**, 123–130.
165 S. Ray, C. A. Pujol, E. B. Damonte and B. Ray, *Carbohydr. Polym.*, 2015, **131**, 315–321.
166 M. Pérez Recalde, M. J. Carlucci, M. D. Noseda and M. C. Matulewicz, *Phytochemistry*, 2012, **73**, 57–64.
167 Z. Wang, J. Xie, Y. Yang, F. Zhang, S. Wang, T. Wu, M. Shen and M. Xie, *Sci. Rep.*, 2017, **7**, 40402.
168 M. Tabarsa, G. M. Park, I. S. Shin, E. Lee, J. K. Kim and S. You, *Mar. Biotechnol.*, 2015, **17**, 266–276.
169 X. Wang, S. Wang, Y. Li, F. Wang, X. Yang and J. Yao, *Int. J. Biol. Macromol.*, 2013, **60**, 248–252.
170 P. Li, X. Zhang, Y. Cheng, J. Li, Y. Xiao, Q. Zhang, A. Zong, C. Zhong and F. Wang, *Carbohydr. Polym.*, 2014, **102**, 852–861.
171 A. S. Vercoutter-Edouart, G. Dubreucq, B. Vanhoecke, C. Rigaut, F. Renaux, L. Dahri-Correia, J. Lemoine, M. Bracke, J. C. Michalski and J. Correia, *Biomaterials*, 2008, **29**, 2280–2292.
172 H. C. Hemker and S. Beguin, *Thromb. Haemostasis*, 1993, **70**, 724–728.
173 S. J. Paluck, T. H. Nguyen and H. D. Maynard, *Biomacromolecules*, 2016, **17**, 3417–3440.
174 K. A. Bauer, D. W. Hawkins, P. C. Peters, M. Petitou, J.-M. Herbert, C. A. A. Boeckel and D. G. Meuleman, *Cardiovasc. Drug Rev.*, 2006, **20**, 37–52.
175 R. C. Sawant, Y. J. Liao, Y. J. Lin, S. S. Badsara and S. Y. Luo, *RSC Adv.*, 2015, **5**, 19027–19033.
176 S. U. Hansen, G. J. Miller, M. Barath, K. R. Broberg, E. Avizienyte, M. Helliwell, J. Raftery, G. C. Jayson and J. M. Gardiner, *J. Org. Chem.*, 2012, **77**, 7823–7843.
177 S. U. Hansen, G. J. Miller, G. C. Jayson and J. M. Gardiner, *Org. Lett.*, 2013, **15**, 88–91.
178 M. Petitou and C. A. van Boeckel, *Angew. Chem., Int. Ed.*, 2004, **43**, 3118–3133.
179 P. Duchaussoy, P. S. Lei, M. Petitou, P. Sinaÿ, J. C. Lormeau and J. Choay, *Bioorg. Med. Chem. Lett.*, 1991, **1**, 99–102.
180 M. Petitou, G. Jaurand, M. Derrien, P. Duchaussoy and J. Choay, *Bioorg. Med. Chem. Lett.*, 1991, **1**, 95–98.
181 T. Li, H. Ye, X. Cao, J. Wang, Y. Liu, L. Zhou, Q. Liu, W. Wang, J. Shen, W. Zhao and P. Wang, *ChemMedChem*, 2014, **9**, 1071–1080.
182 X. Dai, W. Liu, Q. Zhou, C. Cheng, C. Yang, S. Wang, M. Zhang, P. Tang, H. Song, D. Zhang and Y. Qin, *J. Org. Chem.*, 2016, **81**, 162–184.
183 Y. Ding, V. Prasad, V. N. S. Chamakura, H. Bai and B. Wang, *Bioorg. Med. Chem. Lett.*, 2017, **27**, 2424–2427.
184 A. Manikowski, A. Kozioł and E. Czajkowska-Wojciechowska, *Carbohydr. Res.*, 2012, **361**, 155–161.
185 A. Kozioł, A. Lendzion-Paluch and A. Manikowski, *Org. Process Res. Dev.*, 2013, **17**, 869–875.
186 G. Q. Zhang, H. Jin, Y. Zhao, L. Guo, X. Gao, X. Wang, S. Tie, J. Shen, P. G. Wang, H. Gan, H. Cui and W. Zhao, *Eur. J. Med. Chem.*, 2017, **126**, 1039–1055.
187 W. Wildt, H. Kooijman, C. Funke, B. Ustun, A. Leika, M. Lunenburg, F. Kaspersen and E. Kellenbach, *Molecules*, 2017, **22**, 1362–1375.
188 M. Petitou, P. Duchaussoy, J. M. Herbert, G. Duc, M. El Hajji, J. F. Branellec, F. Donat, J. Necciari, R. Cariou, J. Bouthier and E. Garrigou, *Semin. Thromb. Hemostasis*, 2002, **28**, 393–402.
189 J. Choay, J.-C. Jacquinet, J.-C. Lormeau, M. Nassr, M. Petitou and P. Sinay, *US Pat.*, US4818816A, 1989.
190 C. A. A. van Boeckel, T. Beetz, M. Petitou, N. V. Akzo and S. A. Sanofi, *Eup Pat.*, EP0300099A1, 1987.
191 D. J. Langeslay, R. P. Young, S. Beni, C. N. Beecher, L. J. Mueller and C. K. Larive, *Glycobiology*, 2012, **22**, 1173–1182.
192 C. N. Beecher and C. K. Larive, *Anal. Chem.*, 2015, **87**, 6842–6848.
193 M. Hricovini, *J. Phys. Chem. B*, 2015, **119**, 12397–12409.
194 M. Ragazzi, D. R. Ferro, B. Perly, P. Sinay, M. Petitou and J. Choay, *Carbohydr. Res.*, 1990, **195**, 169–185.
195 J. W. Cheng, *Clin. Ther.*, 2002, **24**, 1757–1769.
196 J. M. Walenga, W. P. Jeske, M. M. Samama, F. X. Frapaise, R. L. Bick and J. Fareed, *Expert Opin. Invest. Drugs*, 2002, **11**, 397–407.
197 P. Westerduin, C. A. A. van Boeckel, J. E. M. Basten, M. A. Broekhoven, H. Lucas, A. Rood, H. van der Heijden, R. G. M. van Amsterdam, T. G. van Dinther, D. G. Meuleman, A. Visser, G. M. T. Vogel, J. B. L. Damm and G. T. Overklift, *Bioorg. Med. Chem.*, 1994, **2**, 1267–1280.
198 J. M. Herbert, M. Petitou, J. C. Lormeau, R. Cariou, J. Necciari, H. N. Magnani, P. Zandberg, R. G. M. van Amsterdam, C. A. A. van Boeckel and D. G. Meuleman, *Cardiovasc. Drug Rev.*, 1997, **15**, 1–26.
199 J. Lormeau and J. Herault, *Thromb. Haemostasis*, 2018, **74**, 1474–1477.
200 A. Smogorzewska, J. T. Brandt, W. L. Chandler, M. T. Cunningham, T. E. Hayes, J. D. Olson, K. Kottke-Marchant and E. M. Van Cott, *Arch. Pathol. Lab. Med.*, 2006, **130**, 1605–1611.
201 C. Chen and B. Yu, *Bioorg. Med. Chem. Lett.*, 2009, **19**, 3875–3879.
202 M. Herczeg, E. Mezo, L. Lazar, A. Fekete, K. E. Kover, S. Antus and A. Borbas, *Tetrahedron*, 2013, **69**, 3149–3158.
203 M. Herczeg, E. Mezo, D. Eszenyi, S. Antus and A. Borbas, *Tetrahedron*, 2014, **70**, 2919–2927.
204 G. Lopatkiewicz, S. Buda and J. Mlynarski, *J. Org. Chem.*, 2017, **82**, 12701–12714.
205 S. T. Olson, R. Swanson and M. Petitou, *Blood*, 2012, **119**, 2187–2195.
206 E. Mezo, D. Eszenyi, E. Varga, M. Herczeg and A. Borbas, *Molecules*, 2016, **21**, 1497–1515.
207 J. Harenberg, *Thromb. Haemostasis*, 2009, **102**, 811–815.
208 D. Budragchaa, S. Bai, T. Kanamoto, H. Nakashima, S. Han and T. Yoshida, *Carbohydr. Polym.*, 2015, **130**, 233–242.
209 R. Pauwels, J. Balzarini, M. Baba, R. Snoeck, D. Schols, P. Herdewijn, J. Desmyter and E. De Clercq, *J. Virol. Methods*, 1988, **20**, 309–321.
210 N. S. Gandhi and R. L. Mancera, *Glycobiology*, 2009, **19**, 1103–1115.
211 M. Agostino, N. S. Gandhi and R. L. Mancera, *Glycobiology*, 2014, **24**, 840–851.

212 N. V. Sankaranarayanan, A. Sarkar, U. R. Desai and P. D. Mosier, *Methods Mol. Biol.*, 2015, **1229**, 289–314.
213 N. V. Sankaranarayanan and U. R. Desai, *Glycobiology*, 2014, **24**, 1323–1333.
214 B. Nagarajan, N. V. Sankaranarayanan, B. B. Patel and U. R. Desai, *PLoS One*, 2017, **12**, e0171619.
215 N. V. Sankaranarayanan, T. R. Strebel, R. S. Boothello, K. Sheerin, A. Raghuraman, F. Sallas, P. D. Mosier, N. D. Watermeyer, S. Oscarson and U. R. Desai, *Angew. Chem.*, 2017, **129**, 2352–2357.
216 N. J. Patel, C. Sharon, S. Baranwal, R. S. Boothello, U. R. Desai and B. B. Patel, *Oncotarget*, 2016, **7**, 84608–84622.
217 D. R. Pattabiraman and R. A. Weinberg, *Nat. Rev. Drug Discovery*, 2014, **13**, 497–512.
218 T. Reya, S. J. Morrison, M. F. Clarke and I. L. Weissman, *Nature*, 2001, **414**, 105–111.
219 H. Clevers, *Nat. Med.*, 2011, **17**, 313–319.
220 J. L. de Paz, C. Noti and P. H. Seeberger, *J. Am. Chem. Soc.*, 2006, **128**, 2766–2767.
221 O. J. Plante, E. R. Palmacci and P. H. Seeberger, *Science*, 2001, **291**, 1523–1527.
222 H. A. Orgueira, A. Bartolozzi, P. Schell, R. E. Litjens, E. R. Palmacci and P. H. Seeberger, *Chem. – Eur. J.*, 2003, **9**, 140–169.
223 S. G. Lee, J. M. Brown, C. J. Rogers, J. B. Matson, C. Krishnamurthy, M. Rawat and L. C. Hsieh-Wilson, *Chem. Sci.*, 2010, **1**, 322–325.
224 C. Gao, R. Fujinawa, T. Yoshida, M. Ueno, F. Ota, Y. Kizuka, T. Hirayama, H. Korekane, S. Kitazume, T. Maeno, K. Ohtsubo, K. Yoshida, Y. Yamaguchi, B. Lepenies, J. Aretz, C. Rademacher, H. Kabata, A. E. Hegab, P. H. Seeberger, T. Betsuyaku, K. Kida and N. Taniguchi, *Am. J. Physiol.: Lung Cell. Mol. Physiol.*, 2017, **312**, L268–L276.
225 H. Xu, H. Kurihara, T. Ito, H. Kikuchi, K. Yoshida, H. Yamanokuchi and A. Asari, *J. Biol. Chem.*, 2005, **280**, 20879–20886.
226 R. A. Holloway and L. E. Donnelly, *Curr. Opin. Pulm. Med.*, 2013, **19**, 95–102.
227 K. Shirato, C. Gao, F. Ota, T. Angata, H. Shogomori, K. Ohtsubo, K. Yoshida, B. Lepenies and N. Taniguchi, *Biochem. Biophys. Res. Commun.*, 2013, **435**, 460–465.
228 A. B. Kummarapurugu, D. K. Afosah, N. V. Sankaranarayanan, R. Navaz Gangji, S. Zheng, T. Kennedy, B. K. Rubin, J. A. Voynow and U. R. Desai, *J. Biol. Chem.*, 2018, **293**, 12480–12490.
229 N. V. Rao, B. Argyle, X. Xu, P. R. Reynolds, J. M. Walenga, M. Prechel, G. D. Prestwich, R. B. MacArthur, B. B. Walters, J. R. Hoidal and T. P. Kennedy, *Am. J. Physiol.: Cell Physiol.*, 2010, **299**, C97–C110.
230 K. L. Griffin, B. M. Fischer, A. B. Kummarapurugu, S. Zheng, T. P. Kennedy, N. V. Rao, W. M. Foster and J. A. Voynow, *Am. J. Respir. Cell Mol. Biol.*, 2014, **50**, 684–689.
231 A. B. Kummarapurugu, S. Zheng, J. Ledford, S. Karandashova and J. A. Voynow, *Am. J. Respir. Cell Mol. Biol.*, 2018, **58**, 126–128.
232 S. Zheng, A. B. Kummarapurugu, D. K. Afosah, N. V. Sankaranarayanan, R. S. Boothello, U. R. Desai, T. Kennedy and J. A. Voynow, *Am. J. Respir. Cell Mol. Biol.*, 2017, **56**, 90–98.
233 T. Bonaldi, F. Talamo, P. Scaffidi, D. Ferrera, A. Porto, A. Bachi, A. Rubartelli, A. Agresti and M. E. Bianchi, *EMBO J.*, 2003, **22**, 5551–5560.
234 I. Craciun, A. M. Fenner and R. J. Kerns, *Glycobiology*, 2016, **26**, 701–709.
235 Z. Liu, Y. Jiao, Y. Wang, C. Zhou and Z. Zhang, *Adv. Drug Delivery Rev.*, 2008, **60**, 1650–1662.
236 M. Swierczewska, H. S. Han, K. Kim, J. H. Park and S. Lee, *Adv. Drug Delivery Rev.*, 2016, **99**, 70–84.
237 A. Hedari, H. Namazi and F. Fathi, Nanoparticles Based on Modified Polysaccharides, *The Delivery of Nanoparticles*, InTech, Rijeka, 2012.
238 T. A. Debele, S. L. Mekuria and H. C. Tsai, *Mater. Sci. Eng., C*, 2016, **68**, 964–981.
239 R. Barbucci, R. Rappuoli, A. Borzacchiello and L. Ambrosio, *J. Biomater. Sci., Polym. Ed.*, 2000, **11**, 383–399.